1-1-2010

Investigation of Bone Density Evolution Before and After Total Knee Arthroplasty Using a Thermodynamic-Based Framework

Saeid Nazgooei
Ryerson University

INVESTIGATION OF BONE DENSITY EVOLUTION BEFORE AND AFTER TOTAL KNEE ARTHROPLASTY USING A THERMODYNAMIC-BASED FRAMEWORK

by

Saeid Nazgooei
B.Eng. (Mechanical Engineering)
University of Tehran

A Thesis
Presented to Ryerson University
in partial fulfilment of the
requirements for the
Degree of Master of Applied Science
in the Program of
Mechanical Engineering

Toronto, Ontario, Canada, 2010

Author's Declaration

I hereby declare that I am the sole author of this thesis.

I authorise Ryerson University to lend this thesis to other institutions of individuals for the purpose of scholarly research.

I further authorise Ryerson University to reproduce this thesis by photocopying or by other means, in total or in part, at the request of other institutions or individuals for the purpose of scholarly research.

Acknowledgements

I would like to acknowledge my academic supervisor Dr. Habiba Bougherara, whose support and advice were immeasurable. I don't know how I can adequately express my gratitude to her for being a constant motivator. Her perspective, guidance, and encouragement have been invaluable to my professional and scientific development. I will always be grateful for the opportunity to have worked with such a distinguished leader in the field of biomechanics.

Special thanks to Dr. Seyed M. Hashemi, for his instruction in Adanced Solid Mechanics and Finite Element Methods, which greatly prepared my understanding and competence in the field.

I also owe special thank to professor Leong and professor Stewart for rcommending me to the school of Graduate Studies. I never forget their kindness.

Special thanks to my friend and colleague Mr. Alireza Sayyidmousavi for his prompt assistance in times of need.

I would also like to thank Ms. Leah Rogan, and the School of Graduate Studies at Ryerson University, for their assistance throughout the course of my post-graduate studies.

Most deeply, I thank my wife, Dr. Maria Kalantarian M.D., for her guidance, unconditional support, and friendship over the years. Through her example, I came to believe that I could, with God's help, accomplish any task to which I set my mind and hand.

This page is intentionally left blank.

Abstract

INVESTIGATION OF BONE DENSITY EVOLUTION BEFORE AND AFTER TOTAL KNEE ARTHROPLASTY USING A THERMODYNAMIC-BASED FRAMEWORK

Saeid Nazgooei, B.Sc. Engineering

A thesis presented to Ryerson University in partial fulfillment of the requirements for the degree of Master of Applied Science in the program of Mechanical Engineering

Toronto, Ontario, Canada, 2010

In this study, a new bone remodeling model which combines mechanical loading and bone metabolism factors is used to predict the evolution of bone density after Total Knee Arthroplasty (TKA). A 3D finite element (FE) model of the distal femoral bone, coupled with a new thermodynamic-based theory (BRT), was developed in ANSYS. An axial load of 3000N was applied to the FE model, and the bone density distribution in the femoral bone was calculated. The results were then compared with those obtained from the strain energy density (SED) model and the clinical observations. This comparison showed that the bone density distribution predicted by the thermodynamic-based model before and after TKA is consistent with the structure of the distal femur obtained from X-rays. Furthermore, the predicted bone density distribution using BRT showed a gradual and uniform evolution contrary to the SED model, where there is no gradual bone density evolution.

Table of Contents

List of Figures

List of Tables

List of Medical Terminology

Abduction	outward movement, away from the median axis of the body
Adduction	inward movement, towards the median axis of the body
Arthritis	acute or chronic inflammation of a joint, often accompanied by pain and structural changes and having diverse causes, as infection, crystal deposition, or injury
Arthroplasty	the surgical repair of a joint or the fashioning of a movable joint, using the patient's own tissue or an artificial replacement
Articular	of or related to the joints
Biomimetic	imitating biology and/or living tissue
Cancellous Bone	spongy bone tissue
Condylar	Of or related to the condyles in the distal femur or proximal tibia
Cortical	hard, compact bone tissue
CT or CAT	computer tomography or computed axial tomography; an X-ray technique for producing cross-sectional image of the body
Diarthrosis	freely movable joint, synovial joint
Distal	situated away from the point of origin or attachment, as of a limb or bone; terminal
Femur	thighbone; a bone in the human leg extending from the pelvis to the knee, that is the longest, largest, and strongest in the body
Lateral	direction away from the midline of the body or the sagittal plane
Medial	inward direction towards the midline of the body
Osteoarthritis	the most common form of arthritis, usually occurring after middle age, marked by chronic breakdown of cartilage in the joints leading to pain, stiffness, and swelling.
Osteolysis	dissolution or degeneration of bone tissue through disease
Osteoporosis	increase in bone porosity and subsequent decrease in bone density through disease; usually occurs after osteopenia
Prosthesis	an implant; a device, either external or implanted, that substitutes for or supplements a missing or defective part of the body

Proximal	situated toward the point of origin or attachment, as of a limb or bone
Resorption	dissolution or removal of a substance; e.g. bone tissue
Sagittal plane	a longitudinal plane that divides the body of a bilaterally symmetrical animal into right and left sections
Synarthrosis	immovable joint
Synovial	belonging to, or related to the synovial joint or diarthrosis (*see* diarthrosis)
Tibia	shinbone; the inner of the two bones of the leg, that extend from the knee to the ankle and articulate with the femur and the talus
Tibiofemoral	related to the tibia and the femur
Unicondylar	of or related to only one condyle

List of Abbreviations

ACL	Anterior Cruciate Ligament
ASTM	American Society of Testing and Materials
BMD	Bone Mineral Density
CIHI	Canadian Institute for Health Information
CJRR	Canadian Joint Replacement Registry
CoCrMo	Cobalt-Chromium-Molybdenum Alloy
CT	Computer Tomography, or Computed Axial Tomography (CAT)
DICOM	Digital Imaging and Communications in Medicine
FEA	Finite Element Analysis
OA	Osteoarthritis
PCA	Porous Coated Anatomical
PCL	Posterior Cruciate Ligament
THA	Total Hip Arthroplasty
TJA	Total Joint Arthroplasty
TKA	Total Knee Arthroplasty
UHMWPE	Ultra High Molecular Weight Polyethylene

Nomenclature

Latin

A	Affinity
B	Remodeling
D	Influence of dynamical loading
d	Rate of deformation tensor
E	Elastic modulus / Modulus of elasticity / Young's modulus
F	External force
G	Shear modulus
H	Efficiency of interaction
i	Element index
J	Flux
k	Site-specific reference
L	Onsager phenomenological coefficient
m	Mass
N	Rate of concentration
n	Concentration of reactants
p	Pressure
Q	Heat
q	Coupling parameter
R	Reactant
S	Entropy
s	Threshold level
T	Temperature
t	Second
U	Strain energy density
V	Volume
v	Stoichiometrical coefficient
W	Work
X	Gradient force

x	Displacement
y	Entropy source density

Greek

Δ	Change in a property; usually followed by the notation of the property
ε	Strain
$\mu\varepsilon$	Microstrain ($\varepsilon \times 10^{-6}$)
v	Poisson's ratio
ρ	Density
σ	Stress
F	Muscle force
ψ	Electric potential
μ	Chemical potential
ω	Chemical reaction rate
δ	The ratio of rate of reactions
β	Sum of initial concentration
U	Sum of kinetic, potential, and internal energies

CHAPTER 1 INTRODUCTION

1.1 Background

Bone is a remarkable material having unique material properties and has, like almost all biological tissue, the ability to repair itself and adapts to its mechanical environment by biological remodeling and turnover. With aging, disuse or after prosthesis implantation, bone tissue will resorb, resulting in substantial loss of tissue stiffness and strength [1]. Therefore, it is important to predict this bone resorption after any surgical procedure to avoid a possible revision surgery or the fracture of the femur.

The primary function of the skeletal system is to provide force and motion for mobility in daily living, as well as to protect the vital organs. As bones break, joints wear out and disease may independently make skeletal elements fail, deep understanding of bone remodeling is a key factor to find the optimum way to restore the normal function of the bone by selecting the appropriate design [2]. Abnormal loading and trauma that produces one-time loads that exceed the strength of the bone may lead to bones fracture. Sometimes, cyclic loading is the cause of fracture though the loads never exceed the ultimate strength of the bone. That is because the bone has not yet adapted to increased activity. Bone fracture may also happen under normal loads if the strength of the bone has decreased due to bone tumors or diseases such as osteoporosis. Bone remodeling takes place when loads on the bones are increased or decreased. When loads on the bone are reduced, e.g., prolonged bed rest or during space flight, the ability of the bone to sustain normal loads decreases. Also, in the presence of an implant, the loading on the bone may be decreased. Therefore, bone tissue adapts its geometry and material properties to a smaller portion of the bone and, as a result, again the sustainability of normal loads of the bone will be decreased [1].

The bone remodeling process has attracted the attention of researchers since the bone functional adaptation law proposed by Wolf in the 19^{th} century. It is a coupled process in which old bone is removed (resorption) and new bone is formed in place. Remodeling enables the bone to meet the mechanical demands placed on it [3, 4]. The process begins at an inactive bone surface with bone resorbing cells called *osteoclasts.* After resorptive process, bone forming cells, called *osteoblasts*, appear at the same surface and then new bone is formed by them [5] (Fig. 1.1).

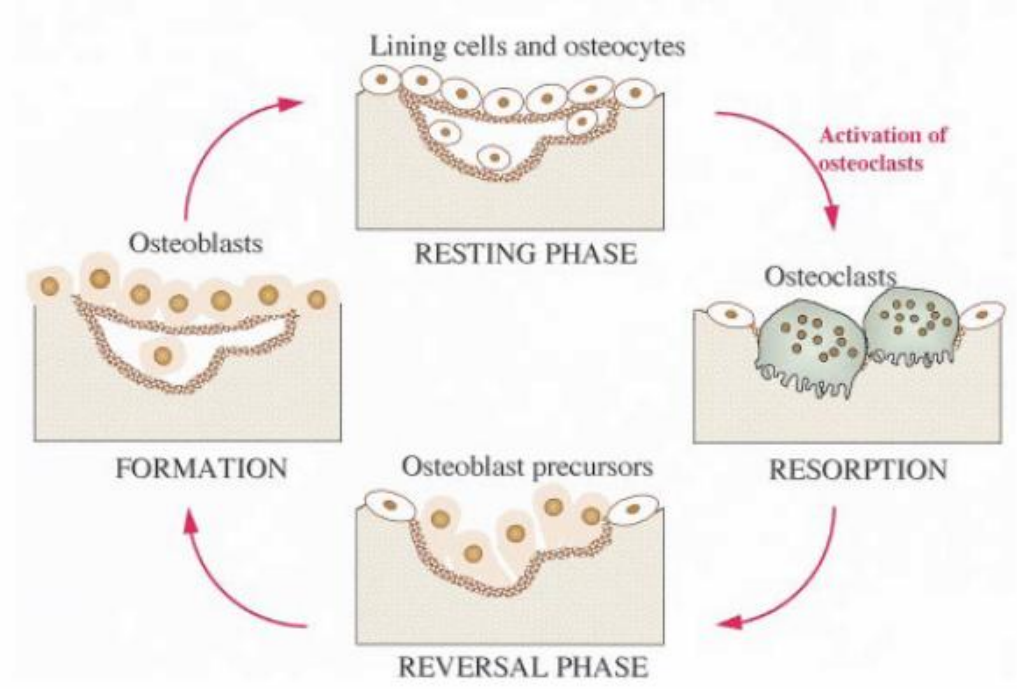

Fig. 1.1: Stages of bone remodeling [3]

Total joint arthroplasty (TJA) changes mechanical loading of the joint. As it mentioned before, bone around the TJA adjusts its density and structure to converge new mechanical demands. Most researchers believe that there is a big decrease in bone mineral density (BMD), adjacent to the implant after TJA. Stress shielding and wear are the main reasons of the prosthesis-related bone loss [6, 7]. Among them, stress shielding, which is a mechanical phenomenon happening in structures including stiff and more flexible materials, is considered as the main reason for loosening implants in TJA [8]. According to this phenomenon, if load is applied to the bone, it grows more tissue in the loaded places; as a result bone becomes stronger to sustain the increased load. On the other hand, in places with decreased load the skeleton makes only so much bone that is necessary to bear the decreased load. Therefore, the bone in this area is weaker [9]. As the bone bears diminished load in the presence of the implant than it borne before surgery, it adjusts itself to the new mechanical situation by diminishing its density [10]. The foregoing bone remodeling process shows living bone tissue tendency of resorption when they are not used.

Implant loosening is created by the loss of surrounding bone tissue causing interface micromotions [11, 12]. Due to stress shielding, osteolysis does not end and bone loss continues; as the bone density decreases, the relative strength of the implant material increases causing the

implant to sustain more load, thereby more decomposing the bone tissue [1]. This cycle of bone loss leads to patient pain and as a result revision surgery. Knee implant involve two bones – distal femur (the bottom end of the femur), and proximal tibia (the upper end of the tibia). It has three components; femoral, tibial, and patellar components (Fig. 1.2).

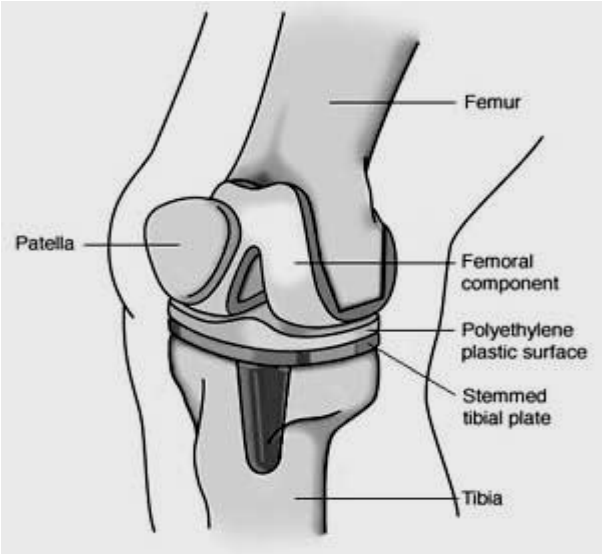

Fig. 1.2: Knee implant components [13]

Femoral component has a convex shape which is a large plate bent to help the curvatures of the femoral condyles (located at distal femur) (Fig. 1.2). This plate is often fabricated from Cobalt-Chromium (CoCr) alloy. The tibial component is a plate made of ultra high molecular weight polyethylene (UHMWPE). This plate is enclosed in a stemmed metallic back-up which is often made of Titanium. Patellar component is fabricated from polyethylene which have a metallic back-up as well (Fig. 1.2). Many different factors contribute to osteolysis after knee arthroplasty [14, 15, 16], but stress shielding has a prominent role in osteolysis in the distal femur [9, 17, 18] and proximal tibia [19, 20].

An enormous number of items play an important role in bone remodeling, such as gender, age, diseases and the individual metabolism [17]. These items make this phenomenon too complex. Therefore, this study will focus on bone's internal structural changes in reply to an alteration in the mechanical and biochemical environments.

As mentioned above, in the presence of implant, bone remodeling should be paid extra attention in clinical and design processes of implant environments. The relationship between bone

structure and mechanical forces has been explained by several models that may be categorized in three groups: mechanical, mechanobiological, and biochemical models [21].

In mechanical models, it is assumed that the bone structure relates to mechanical loads. Although these models were able to predict changes in the bone structure, they have limited the stimuli that cause changes in the bone structure to mechanical stimuli such as stress, strain and strain energy density [22]. Also, these models consider just the geometry and material properties of the bone and prosthesis to achieve a quantitative prediction of bone structure after implantation relative to intact bone [11].

Mechanobiological approach to bone form and function was proposed first by Frost [23]. According to this model, there is a *minimum effective strain* (MES) that is considered as a very low level of strain. Strains under the MES would make bone cells resorption and strains over the MES would prevent the resorption. During normal activities, strains would not exceed the MES and bone structure does not need to adjust strains smaller than MES [24].

The biochemical bone remodeling models are based on the osteoclasts and osteoblasts activities. In these models, some hormones are considered as stimuli for bone resorption and formation. Also, receptor activator of proteins and genes has a very important role in bone remodeling. Although these models consider metabolic factors as chemical stimuli, which are very important to improve the understanding of bone remodeling, the key role of mechanical stimuli has not been taken into account [21].

Recently, a thermodynamic-based model for bone remodeling has been proposed by Bougherara *et al.* [21]. This model is based on irreversible thermodynamics principles, in which the mechanical factors are linked to the bone-metabolism. As this model is cell-based, it provides better understanding of bone resorption and formation at the cellular level and also gives some insights into bone diseases such as bone tumours, osteoporosis, and osteopenia and so on. Practically, this thermodynamic-based model will be used to predict the evolution of bone density after knee arthroplasty in order to improve the overall design of knee implants.

The main objective of this study is to predict the evolution of bone density in a simulated distal femoral bone before and after total knee arthroplasty (TKA) using the thermodynamic-based model of bone remodeling, and compare the results of the numerical simulations to clinical data. The model will also be compared to the classical bone remodeling theory that uses the strain energy density to predict bone loss.

1.2 Motivation

Osteoarthritis and related conditions represent a large group of diseases affecting the joints, ligaments, tendons, bones and other constituents of the musculoskeletal system. These conditions are highly common and are the main causes of morbidity, disability, and health care utilization. As a treatment for arthritis, knee replacements have been showing great success in relieving pain, increasing independency in patients who do not respond to non-surgical therapies, and the procedures are cost effective. According to statistics, the number of knee replacements in 2006-2007 increased by 140% since 1996-1997 (15,829) with a 9% increase compared to the previous year (2005-2006). As the stress field on the surrounding bone is affected by implanted prosthesis, understanding of the relationship between mechanical forces and bone remodeling is important for improving existing prostheses and developing new ones [25].

1.2.1 Arthritis in Canada

In 2005-2006, surgeons were asked to record the most accountable diagnosis applicable to patients for primary knee replacements. Degenerative osteoarthritis was indicated as the most commonly reported responsible diagnosis (93%) followed by inflammatory arthritis (4%) and post-traumatic osteoarthritis (2%). Although degenerative osteoarthritis is determined as the main diagnosis in all age groups, the distribution of the other diagnoses between various age groups is significantly variable. As Fig. 1.3 depicts, degenerative osteoarthritis and inflammatory arthritis has the highest proportion for patients who were 65 to 74 years; post-traumatic has the highest proportion for patients who were 55 to 64 years old; and osteonecrosis has the highest proportion for patients who were 75 to 84 years old [26].

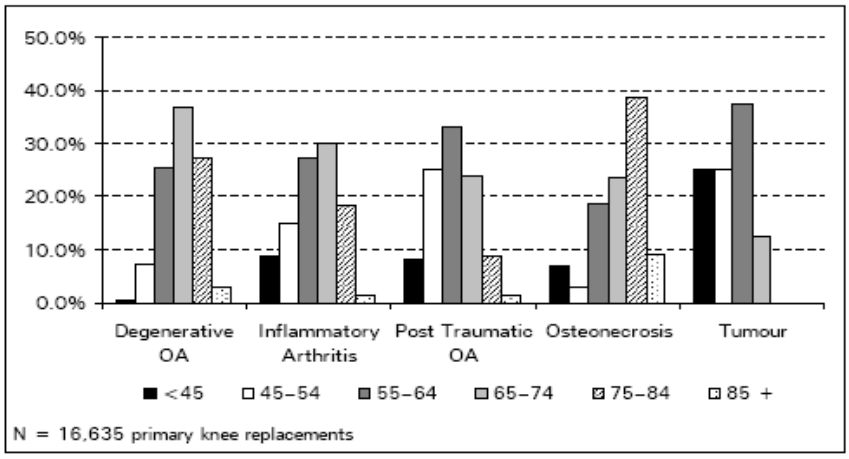

Figure 1.3: Age Distribution by Responsible Diagnosis, Primary Knee Replacements, CJRR, 2005-2006 [26]

1.2.2 Joint replacement in Canada

Knee replacement hospitalizations in Canada have been growing between the fiscal years 1995-1996 and 2006-2007 as Fig. 1.4 depicts. There were 62,196 hospitalizations for hip and knee replacements in Canada, not including Quebec, in 2006-2007, showing a 10-year increase of 101% from 31,043 procedures in 1996-1997 and a one-year increase of 6% from 58,470 procedure in 2005-2006. This one-year increase is less than that observed in the previous year (2005-2006), where the one-year increase was 17%. In 1996-1997, the number of knee replacement slightly exceeded the number of hip replacements in Canada, not including Quebec (15,829 versus 15,214 surgeries, respectively). Since then, the number of knee replacement has increased at a pace greater than that of hip replacements. In 2006-2007, there were 37,943 hospitalizations for knee replacements. The number of knee replacements in 2006-2007 increased by 140% since 1996-1997 (15,829) with a 9% increase compared to the previous year (2005-2006), showing the importance of improvement in implants [26].

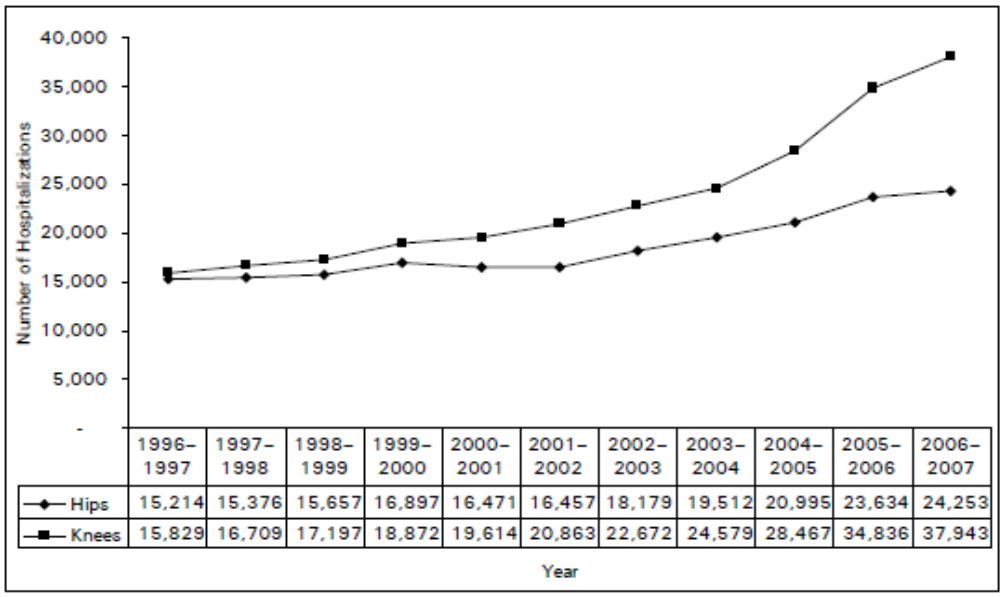

	1996–1997	1997–1998	1998–1999	1999–2000	2000–2001	2001–2002	2002–2003	2003–2004	2004–2005	2005–2006	2006–2007
Hips	15,214	15,376	15,657	16,897	16,471	16,457	18,179	19,512	20,995	23,634	24,253
Knees	15,829	16,709	17,197	18,872	19,614	20,863	22,672	24,579	28,467	34,836	37,943

Fig. 1.4: Number of Hospitalizations for Hip and Knee Replacement Procedures in Canada, 1996-1997 to 2006-2007 [26]

1.2.3 Primary versus revision surgeries

Fig. 1.5 indicates among the knee replacements reported in CJRR for 2006-2007, 93.7% of them involved primary operations and 6.3% of them involved revisions.

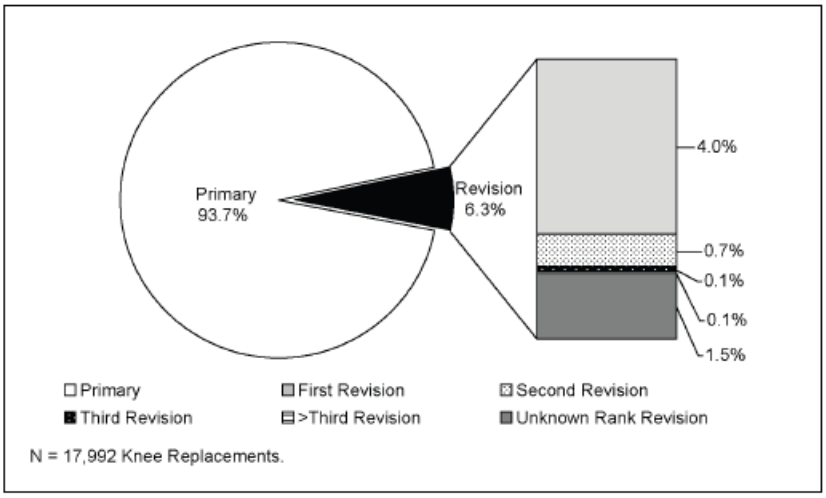

Fig. 1.5: Type of Knee Replacements, CJRR, 2006-2007 [26]

1.3 Knee joint

1.3.1 Knee anatomy

First, some common anatomic terms are going to be defined as they relate to the knee. Many parts of the skeleton are exactly alike. So it is common to determine parts of the skeleton using clause that define where the part is in relation to an imaginary line drawn through the middle of the body. For instance, *medial* means closer to the midline. Therefore, the medial side of the knee is the side that is closest to the other knee and the *lateral* side is the side that away from the other knee. Likewise, *anterior* refers to the front of the knee and *posterior* refers to the back of the knee (Fig. 1.6) [27].

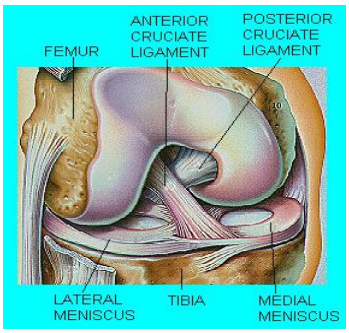

Fig. 1.6: Right knee [27]

The knee joint is a bicondylar articulation in which two important bones meet each other; the *femur* (the thighbone) and the *tibia* (the shinbone), and allows them to rotate, twist, and slide relative to one another [28, 29]. The *patella* or k*neecap*, which is the third bone in the knee joint, sits in front of the knee as Fig. 1.7 depicts [30].

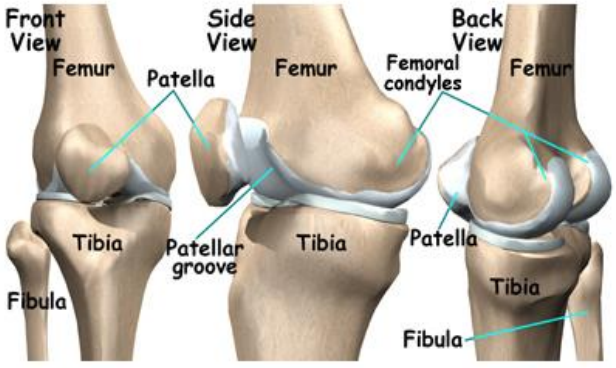

Fig. 1.7: Knee joint from three different views [30].

As the knee joint is lubricated by a fluid called *synovial fluid*, it is considered as a *synovial joint* (Fig. 1.8).

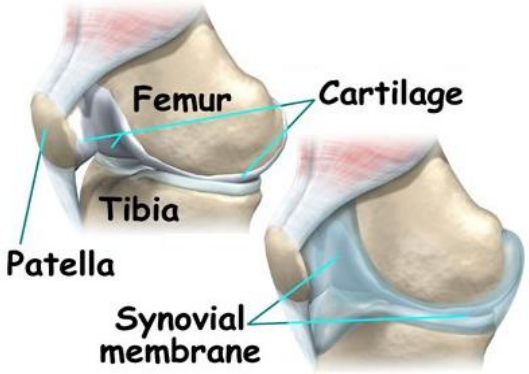

Fig. 1.8: Synovial Joint of the Knee [30].

1.3.2 Bone composition

Bone has four main functions: provide force and motion for mobility and take care of the functions of daily living; protect the vital organs such as the brain, heart, spinal cord, and lungs; act as a mineral bank, especially for calcium and phosphorous; and provide sites for the formation of red blood cells, a process known as hematopoiesis.

Bone tissue is a hierarchical composite at many levels. At the lowest level (~0.1 micron scale), it is a composite of mineralized collagen fibrils. At the highest hierarchical level (1-2 mm), there are two types of bone: (1) *cortical* bone which comes as tightly packed lamellar, Haversian, laminar, or woven bone; and (2) *trabecular* bone, which is a highly porous cellular solid. Cortical, or compact bone, is the densest bone in the skeleton. Cancellous bone, or trabecular or spongy bone, is much less dense than cortical bone. Spongy bone tissue makes up most of the bone tissue of short, flat, and irregularly shaped bones. It also forms most of the epiphyses of long bones and a narrow rim around the modularly cavity of the diaphysis of long bones. Spongy bone tissue is different from compact bone tissue in two respects. First, spongy bone tissue is light, which reduces the overall weight of a bone so that it moves more readily when pulled by a skeletal muscle. Second, the trabeculae of spongy bone tissue support and protect the red bone marrow. Compact bone tissue is arranged in units called *osteons* or *haversian systems*. In

contrast to compact bone tissue, spongy bone tissue does not contain osteons [31]. Figure 1.9 depicts a diagram of the two types of bone.

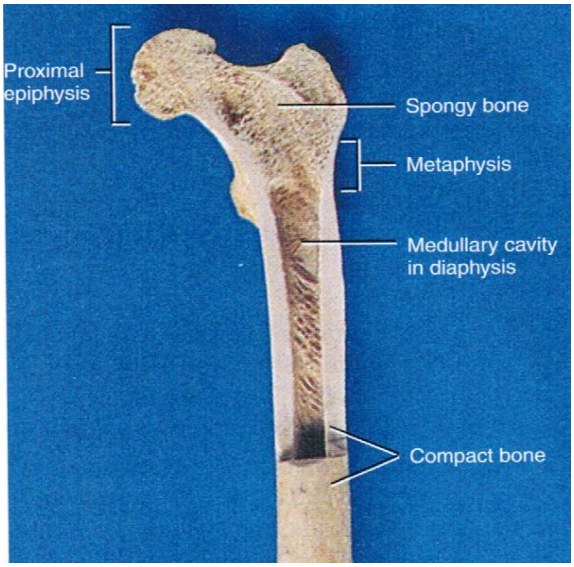

Fig. 1.9: Partially sectioned femur [31].

Volume fraction is the ratio of the volume of actual bone tissue to the bulk volume of the specimen, which includes the volume associated with the vascular pore spaces, but ignores the presence of lacunae and canaliculi. While the volume fraction of cortical bone is greater than about 0.7, the trabecular bone has a volume fraction rarely greater than about 0.6.

Both cortical and trabecular tissues are porous. Porosity of adult human femoral cortical bone, for example, can vary from as low as 5 percent at age 20 up to almost 30 percent at age 80. Porosity of trabecular bone varies from about 50 percent in the young adult femoral head up to about 95 percent in the elderly vertebra.

A variety of measures are used to describe bone density. The most common ones are tissue density and apparent density, which can be obtained for hydrated, dehydrated, or deorganified bone. Tissue density, ρ_{tiss}, is defined as the ratio of mass to volume of the actual bone tissue, not including any vascular porosity. It is similar for hydrated cortical and trabecular bone, varies little, and is about 2.0 g/cm^3. Apparent density, ρ_{app}, is defined as the ratio of the mass of bone tissue to the bulk volume of the specimen, including the volume associated with the vascular pore spaces. The apparent density of cortical bone is about 1.85 g/cm^3 and varies little from site

to site. In contrast, the average apparent density of trabecular bone depends greatly on anatomic site. It is as low as 0.1 g/cm^3 for the elderly spine, about 0.3 g/cm^3 for the human tibia, and up to about 0.5 g/cm^3 for the load-bearing portions of the proximal femur [1].

1.3.3 Cortical bone properties

Cortical, or compact bone, is the densest bone in the skeleton. The diaphysis, or central shaft, of a long bone such as the femur or tibia is made of cortical bone. The longitudinal axis is generally aligned with the diaphyseal axis of long bones. Cortical bone is both stronger and stiffer when loaded in the longitudinal direction, compared with the radial or circumferential directions. This structure efficiently resists the largely uniaxial stresses that develop along the diaphyseal axis during habitual activities such as walking and running.

There is a preferred orientation in the microstructure of bone. In cortical bone, the preferred orientation is determined by the generally parallel assembly of the osteons, whereas in trabecular bone it is determined by a predominant alignment of the plates and rods. As result of this orientation, bone is an anisotropic material. Many biological materials are orthotropic, for which the material behaviour can be described with reference to three mutually perpendicular material axes (principal material axes) at each point. If there is symmetry about any one of the principal material coordinate axes, then the other two axes can be interchanged, and isotropy exists in the corresponding plane of these axes. This is called *transverse isotropy*, since the "transverse" plane is isotropic. Adult human cortical bone, for example, is often considered to be transversely isotropic due to the longitudinal orientation of the osteons which is aligned with the long bones axes. Therefore in the diaphyseal direction, cortical bone is stiffer compared with radial directions [1].

According to Reilly and Burstein [32], a total of five independent material constants are required to describe the transversely isotropic elastic properties of cortical bone (Table 1.1). Also, the longitudinal Young's modulus of human cortical bone is in the range of about 10-22 GPa.

Table 1.1: Average Anisotropic Elastic Properties of Human Femoral Cortical Bone [32]

Cortical elastic properties	Average value
Longitudinal modulus (MPa)	17000
Transverse modulus (MPa)	17000
Shear modulus (MPa)	3300
Longitudinal Poisson's ratio	0.46
Transverse Poisson's Ratio	0.58

1.3.4 Trabecular bone properties

From a biomechanical perspective, the most important microstructural parameter for trabecular bone is its apparent density, in contrast to the tissue density of the individual trabeculae.

The compressive stress-strain behaviour of trabecular bone (Fig. 1.10) is typical of a class of porous materials called cellular solids. It displays an approximately linearly elastic region followed by a local peak, and then a strain-softening or plateau region of near constant stress with increasing strain. Tensile behaviour is much more brittle, with fracture occurring at relatively low strains. Most importantly, for trabecular bone, the stiffness and strength depend on its apparent density and can vary by two orders of magnitude within the same metaphyseal region [33].

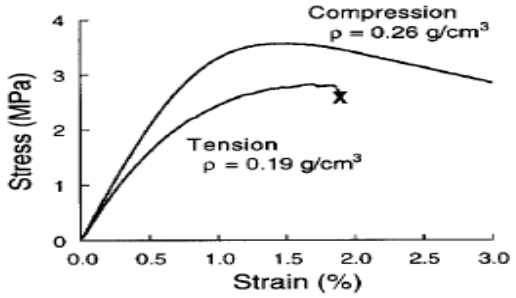

Fig. 1.10: Stress-Strain behaviour of human trabecular bone [33].

Because of the large variation in apparent density for trabecular bone (Table 1.2) its mechanical properties cannot generally be described by average values. This makes analysis of structural problems with trabecular bone more difficult than those for cortical bone, since it is usually necessary to account for variations in apparent density within a region of trabecular bone. However it should be realized that there are substantial variations in the mechanical properties of

trabecular bone across anatomic sites, and efforts should be made to use site- specific average values if available. Table 1.2 gives such properties for the tibia and femur.

Table 1.2: Properties of Bone Cancellous in Proximal Tibia and Distal Femur

Study	Year	Wet Apparent Density (g/cc)		Modulus (MPa)	
		Mean	Range	Mean	Range
Proximal Tibia					
Linde et al. [34]	1989	0.29	0.09-0.66	445	61-1174
Ashman et al. [35]	1989	0.26	0.13-0.75	1107	340-3350
Distal Femur					
Rohlmann et al. [36]	1980	0.5	0.14-1.00	389	44-1531

1.3.5 Human gait

The way in which a human moves by foot is called *gait* [37]. Normal gait is a highly complex activity that we learn it naturally and it is the most energy-efficient method that we use to walk [38]. Some mechanical factors such as joint's loads and orientation during walking may be measured by gait analysis [39]. A gait begins when one foot hits the ground and ends when it hits the ground again (Fig. 1.11).

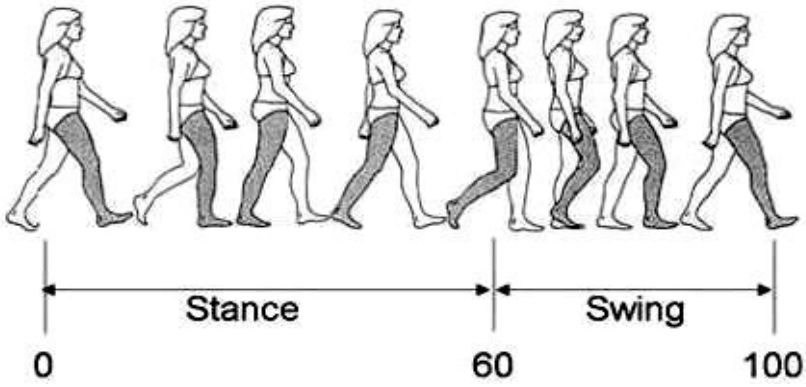

Fig. 1.11: The human walk cycle [40]

The gait cycle may be divided into two phases; *stance*, which is 60% of the cycle and begins with the first contact of the heel with the ground, and *swing* which includes 40% of the gait cycle and begins at toe-off. This ratio changes with walking speed [38, 41]. Opposite heel-strike and toe-off occur at 10% and 50% of the cycle. The stance phase may be divided into five subperiods: initial contact, loading response, midstance, terminal stance, and preswing. Also, swing phase may be divided into three subperiods: initial swing, midswing, and terminal swing.

During the gait cycle, there is two periods of *double support* (or *double limb support*) during which the body's centre of mass is at the lowest level. The foot, during the stance phase, is in contact with the ground and flies during swing phase. Stance phase starts when the foot hits the ground for the first time and the first period of double support is occurred which is called *loading response* during which the shock of impact is absorbed and the body weight is transferred from one leg to the other. The opposite foot aloft and moves behind the knee during *mid-stance* which is approximately 10%-30% into the gait cycle. During 30%-50% into the gait cycle, *terminal stance*, the heel starts rising and the opposite foot hits the ground for the first time. Following terminal stance and during *pre-swing* phase, approximately 50%-60% into the gait cycle, second period of double support is occurred and body weight is transferred to the other leg. The next phase is *initial swing*, 60%-73% into the gait cycle, during which the leg takes off and moves toward the body. During the next phase, *mid-swing* phase which is 73%-87% into the gait cycle, the knee extends and straightens. Finally, swing phase concludes when the foot hits the ground for the second time [37-39, 41, 42].

1.3.6 Motion of the knee

One important issue in understanding normal function and the etiology of various joint diseases is the relationship between the loads on a joint and its motion. This is critical in design of total joint replacements, since historical perspective has shown the importance of reproducing the normal relationship between loads and motion to avoid premature loosening of the components or damage to articulating surfaces. The body appears to be conditioned to apply specific muscle forces about a joint for specific kinematic tasks.

If the joint cannot move in its expected path in response to these loads because of some geometric changes in the system (for example, a damaged meniscus at the knee), the resulting motion may be erratic. Conversely, if the expected loads are not supplied for a given kinematic task due to a disruption of the load bearing tissues such as tendons or ligaments about the joint, it may not be possible to complete the task. In either case, pain can result and function is impaired.

The knee joint has six degrees of freedom; three rotation and three translations (Fig. 1.12). If one considers the femur as fixed and the tibia as moving relative to the femur, the clinically apparent rotations are flexion-extension, internal-external rotation and abduction-adduction (also known as varus-valgus motion). Considering the femur fixed and the tibia moving relative to the femur,

the tibia can translate medial-lateral, anterior-posterior, and distal-proximal [43]. Normal knee flexion ranges from zero degrees (full extension) to 160 degrees in a fully flexed knee. Rotation of the femur about the longitudinal tibial axis also occurs. This is greatest when the knee is flexed and least when the knee is in full extension. Injury or disease may result in the loss of ligament function. For example, if the anterior cruciate ligament is ruptured, anterior motion of the proximal tibia with respect to the femur will increase [43].

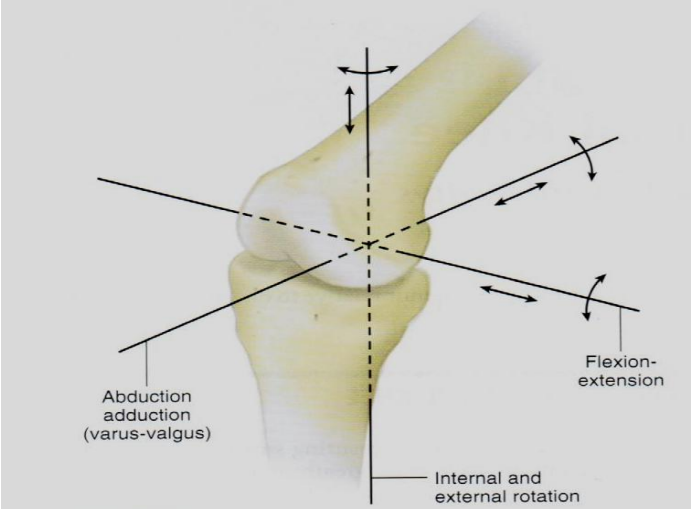

Fig. 1.12: Degrees of freedom of the knee [43].

1.3.7 Loads and moments

Motion analysis has been used to determine the resultant forces and moments acting across the knee joint. Several studies have been conducted to determine the loads that the knee joint experiences during normal gait [44-47]. The peak axial joint load, which approximates the contact force if soft tissue loading is negligible, has been determined to be three to four times bodyweight during normal gait [38]. Therefore, four times body weight is a commonly used value for the femoral-tibial contact force when designing total knee replacement. Denham and Bishop [48] analyzed static force transmission at the knee to obtain the position of the line of body weight correct orientation of the bones of the knee during its function. With their proposed technique it could be suggested values for different forces acting at the knee.

For different daily activities the forces in the knee joint vary largely. Morrison [49] estimated maximum knee joint compressive forces about 4 to 4.5 times body-weight during daily activities. Kuster et al. [50] calculated knee joint loading during both level and downhill walking (Fig.

1.13). They obtained maximum tibiofemoral compressive force about 3.9 times body-weight (BW) for level walking and 8 times BW for downhill walking during the initial stance phase. According to their estimation, during downhill walking 80% and level walking 70% of the maximum bone-on-bone forces are muscle forces, whereas these values for the ground reaction are only 20% and 30% respectively. These values obtained at 20% knee flexion.

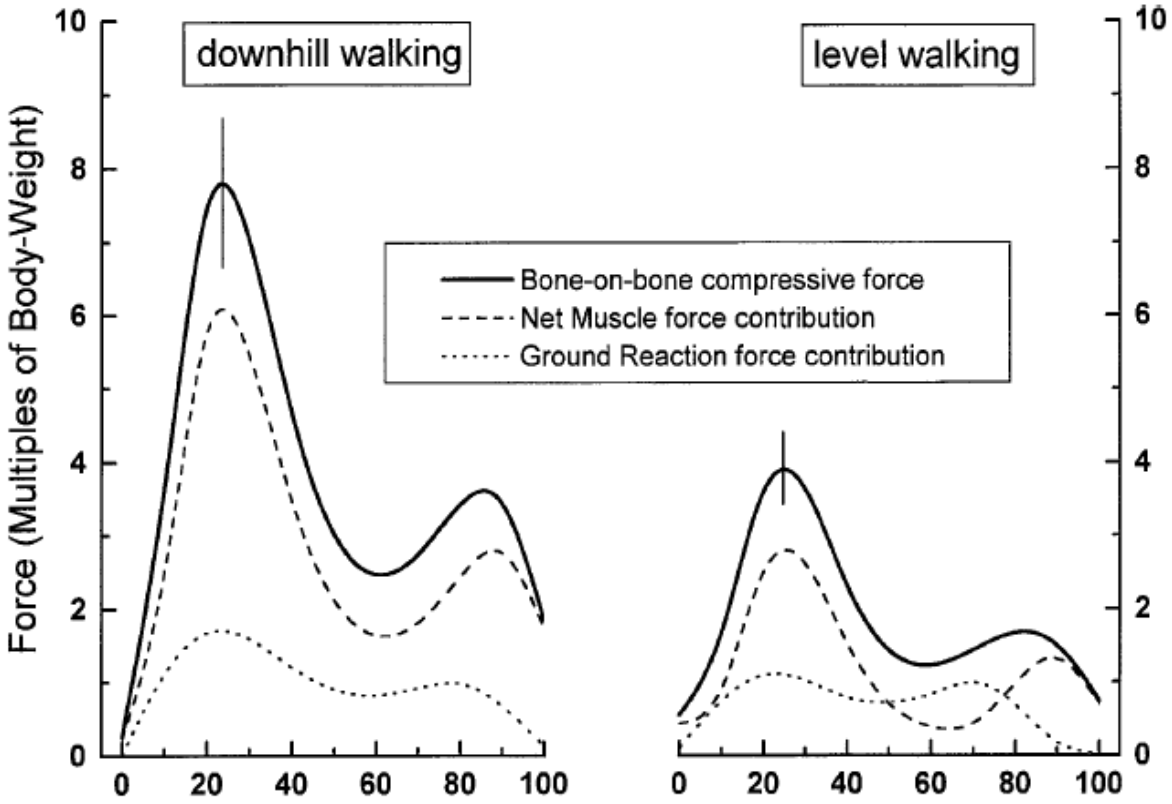

Fig. 1.13: Mean tibiofemoral joint loading during the stance phase [50].

Figure 1.13 depicts the knee joint compressive forces during stance phase in level and downhill walking. The values on the vertical axis are multiples of body-weight (BW) and on the horizontal axis are normalized to 100% of the stance time, meaning heel strike occurs at 0% and toe-off at 100% [50]. Table 1.3 shows reported tibiofemoral joint loads for different daily activities [50].

Since in many previous FEA studies the tibiofemoral axial compressive loads for level walking have been considered 2 to 4 times the body weight (Table 1.3), a 3000 N force is used in this study.

Table 1.3: Tibiofemoral joint loads for different daily activities reported by different researchers [50].

Author(s)	Activity	Tibiofemoral joint load (body-weight multiples)
Ericson and Nisell [51]	Cycling	1.2
Morrison [47]	Level walking	3.0
Harrington [51]	Level walking	3.5
Kuster [50]	Level walking	3.9
Collins [52]	Level walking	3.9 to 6.0
Morrison [49]	Downstairs walking	3.8
Andriacchi [53]	Downstairs walking	6
Morrison [49]	Downhill walking	4.5
Kuster [50]	Downhill walking	8
Ellis [54]	Rising from chair	3.2
Nisell [55]	Isokinetic knee extension at 30^{o}/sec	9
Dahlkvist [56]	Squat descent	5.6
Collins [57]	Weightlifting (120kg)	Up to 24

1.4 Knee replacement

In knee replacements, the goal is to create a bone-implant system that provides normal function for the life of the patient. In knee joints, the problem of providing normal function is somewhat more complex than in hip, because soft tissues provide most of the kinematic constraint. If both contacting surfaces are replaced, knee design is total joint replacement. Most designs are tricompartmental. That is, the surfaces of the tibia, femur, and patella are all replaced. In this chapter knee replacement, their failure and a description of bone loss will be discussed.

Surgeons with some years of experience have noticed that fashion tends to repeat itself. For example, in the early years (1970 to 1974), a range of prostheses (unicondylar, bicondylar, and hinged) were used, depending on the preoperative condition and deformity. For a while these

prostheses didn't use, due to their failure, and tricondylar resurfacing prostheses were in vogue for virtually all procedures. In recent years, successful results have been obtained with unicondylar prostheses in selected patients, and both constrained and hinged prostheses have found a place in the surgical armamentarium for revision and complex primary surgery. Therefore, at this important time in the field of Total Knee Replacement (TKR), as the original pioneers are succeeded by the next generation of surgeons, change should only be included once three criteria have been met: first, a problem that needs a solution should exist; second, the solution should be based on solid basic science research; and finally, the clinical results should be documented by the innovator and others. Therefore, to help guide this pursuit of continuing improvement in Total Knee Arthroplasty (TKA), it is useful to look at what has worked and what has not worked in the past [58].

1.4.1 A history of knee replacement

According to Insall and Clarke, the first improvement in knee joint function by modifying the articular surfaces occurred in 19^{th} century. In 1860, Verneuil introduced the concept of interposition of soft tissue to recover the articular surface of a joint. Pig bladder, nylon, fascia lata, prepatellar bursa, and cellophane were some of the materials used for this purpose [58]. As the results were not good, Ferguson [59] resected the entire knee joint. While the patients enjoyed good motion by removing more bone, spontaneous fusion often resulted by less bone resection. The results of this procedure were sufficiently poor to discourage anything more than occasional attempts in severe cases [58]. In 1940, Campbell [60] used a metallic interposition femoral mold for the first time and the result was relative success. Similar type of arthroplasty was used by Speed and Trout [61] in 1949 and by Miller and Friedman [62] in 1952, but the results were not very good. In 1958, Macintosh [63] inserted acrylic tibial plateau prosthesis into the affected side to correct deformity, restore stability, and relieve pain. McKeever [64, 65, 66] used later version of this prosthesis, which was made of metal and showed considerably more success and was extensively used, particularly in patients with rheumatoid arthritis. After that, Gunston [67] stepped further and used polycentric prosthesis which was the first cemented surface arthroplasty of the knee. He substituted metallic runners embedded in the femoral condyles that articulated against polyethylene attached to the tibial plateau rather than using a simple metal disk interposed within the joint. Parallel to the improvement of interposition and surface replacement, the hinged prosthesis made of metal was developed in 1951 [58]. Early

results were promising, but failures soon appeared as a result of component loosening. McKeever prostheses continued to be implanted in less involved knees, but follow-up showed only 60% good midterm results in the rheumatoid patient [68]. Shiers [69] also described a hinged prosthesis with very simple mechanical characteristics. Technically, a hinged prosthesis is self-aligning and self-stabilizing. Therefore, all the ligaments and other soft-tissue constraints can be eliminated. This makes it considerable appeal [58].

Knee designs can be categorized in several ways. For example, Bartel et al. [1] categorized the designs to bicondylar and unicondylar. In bicondylar designs the surfaces of the tibia, femur, and patella are all replaced, whereas in unicondylar designs only one compartment of the joint (lateral or medial) is affected. Therefore, only surfaces of the femoral condyle and the tibial plateau in the affected compartment are replaced. Insall and Clarke [58] categorized the prosthesis design to surface replacement and constrained design. They subdivided the surface replacement designs to unicondylar and bicondylar designs. Bicondylar may be further subdivided to cruciate retaining, cruciate excising, or cruciate substituting. Constrained prostheses, also, can be subdivided to hinged and unlinked. Figure 1.14 depicts some of the early knee implant designs.

In the late 1960s, knee implant designs were categorized to anatomical and functional [66]. Functional called for sacrifice of both cruciate ligaments (PCL and ACL), whereas the anatomical allowed their preservation. In fact, "Functional designs permitted nonanatomical joint surface geometries intended to maximize surface area and reduce polyethylene stress [70]". Anatomical and functional designs can be subdivided into fixed and rotating platform (or mobile-bearing). During walking, in the fixed knee implant designs, femoral component articulates across a plastic tibial surface, whereas in the mobile-bearing designs both the femoral and tibia components are in motion [66].

Freeman and Swanson used the first functional cemented condylar total knee in the late 1960s [71, 72]. Following that, in 1971, "the first cemented bicondylar knee design preserving the cruciate ligaments [70]" was invented.

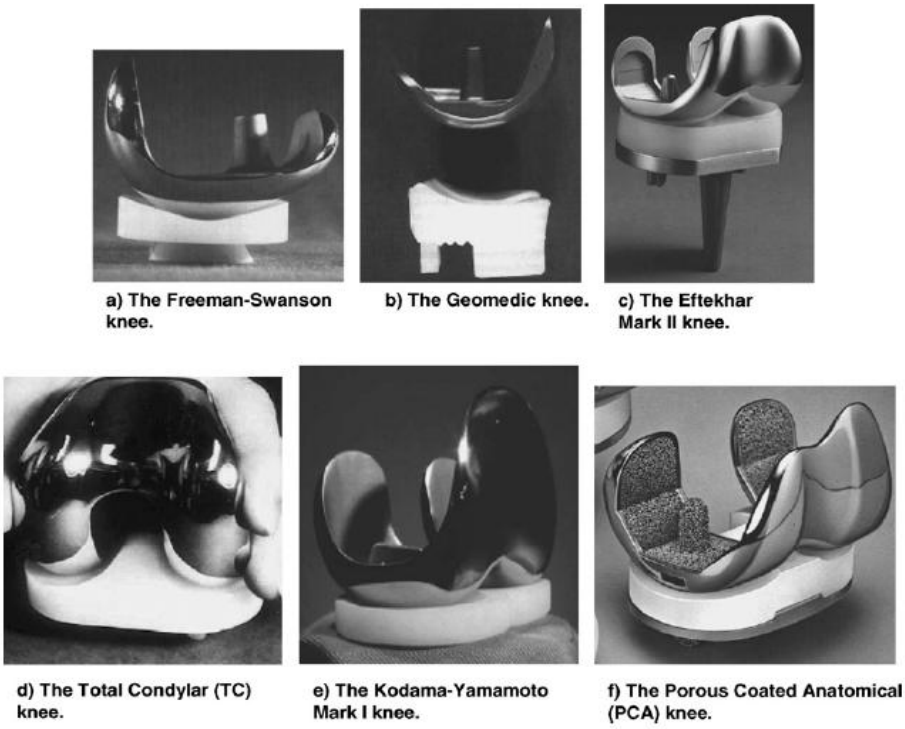

Fig. 1.14: some of the early knee implant designs [66].

Two years later, in 1973, another innovation to knee implant design was introduced. This functional model was called Eftekhar Mark II [66]. In the same year, Total Condylar (TC) knee was created by Robinson as "the first truly successful and widely used functionally designed cruciate-sacrificing implant [70]", but the first cementless total condylar knee have already invented by Yamamoto and Kodama in 1968. It was called Kodama-Yamamoto Mark I knee and was the first anatomical total condylar knee [73]. Ten years later, in 1979, Hungerford, Kenna, and Krackow invented the first porous coated total anatomical (PCA) knee [74].

1.4.2 The Stryker Duracon TS knee implant system

The Duracon knee implant is a knee system in which the femoral and the core tibial materials are made of Cobalt-Chromium-Molybdenum (CoCrMo) alloy, whereas the tibial bearing inserts are made of ultra high molecular weight polyethylene (UHMWPE). This product is manufactured by Stryker Orthopaedics (Stryker Corporation, Kalamazoo, MI, USA) (Fig. 1.15) [75]. Femoral component of Duracon system will be used to generate the CAD model in the chapter 5. The material properties of femoral component of this system will be used in the finite element study discussed in the chapter 6.

Fig. 1.15: The Stryker Duracon TS Knee Implant System[75]

1.4.3 Failure

The resulting bone-implant system is a composite structure consisting of several components that should last for the lifetime of the patient. This is a challenging design problem that must account for the strength of the prosthetic components, damage to the articulating surfaces, and the strength of the interfaces between the implanted materials and the bone, and the potential adaptation of the bone due to altered loading. The basic premise is that joint replacements fail structurally because stresses have exceeded the strength of components, interfaces, or articulating surfaces. Foreign materials employed into the body not only must be biocompatible in a hostile environment, but must tolerate significant biological and mechanical stresses for many years [76-78]. Failure may occur within the prosthetic themselves [79-81], at the implant-bone interfaces [82-84], or in the bone [9, 11, 12, 85, 86].

Cracks or flaws in implant materials do not heal and may be spread with repeated loading. As a result, the fatigue behaviour of metals and polymers used for prosthetic replacements is an important concern [87]. Another major structural consideration is the surface damage that occurs due to contact between the articulating surfaces [79-81]. Well-designed components generally do not wear out, but debris is liberated. The particles from the damaged surfaces collect in the surrounding soft tissue. When sufficient debris accumulates, the biological response of the body can lead to increased risk of infection and increased risk of loosening [29, 76, 79-81, 88, 89].

Beside of these structural reasons of failure of knee implants, localized bone loss induced by stress shielding is another important concern in occurring of failure. Because stress shielding as a

reason of bone resorption and implant loosening after TKA is within the scope of this study, the next section is allocated to this issue and the other causes of implant failure are not covered.

1.4.4 Stress shielding

The bone-implant structure created at surgery is a multicomponent system that replaces the bone alone, which is itself a composite structure consisting of cortical and cancellous bone. The new composite structure consists of cortical and cancellous bone, the implant, and usually an interface layer such as bone cement. These interfaces are complex and vary from simple bony contact, allowing only compressive loads and shear transfer through friction [90], to bony ingrowth interfaces that transfer tensile, compressive and shear loads [91-94]. In some regions, there may be fibrous tissue laid down between the implant and the bone that provides a weaker, less stiff connection between the bone and implant.

According to a mechanical effect, if there is a composite with two materials in which one component is stiffer than the other, the stiffer part bears the greater part of the load. On the other hand, the skeleton in our bodies adapts itself to a new mechanical environment if there is any change in loading. It creates more bone tissue in the places which sustain more loads. As a result, the skeleton will become stronger in the loaded area so that it can sustain the exceeded load. The same scenario occurs when there is a diminishing load, but the skeleton would be weaker in the diminished load areas.

Considering the above discussion, when an artificial joint is used, the load previously carried by the bone alone is now shared by the bone and the implant. Consequently, the amount of load carried by the bone generally is decreased, and the bone will remodel to meet the requirements of the new loading situation, thereby *resorbing* the bone. This phenomenon is known as *stress shielding* [12, 85].

In a composite system with parallel load paths, the load is shared according to the relative stiffness of the components in the composite structure. If, when the implant is in place, the stiffness of the bone decreases due to decreased load, the relative stiffness of the implant with respect to the bone will increase, the load carried by the prosthesis may increase, that carried by the bone may decrease, and a further decrease in stiffness of the bone may occur. Thus, there is the possibility of a vicious cycle, in stemmed components, for example, in which the strength of

the bone and the amount of bone may decrease to the point where the structural integrity of the system is in jeopardy and risk of failure of both the bone and the stem is increased [14, 16]. This phenomenon is called *osteolysis*. Figure 1.16 displays qualitative bone loss anteriorly in the distal femoral condyle due to stress shielding 4 years after TKA [9].

Many follow-up studies have shown there is bone resorption at the anterior distal region of the femoral condyles in which the femoral component that causes stress shielding of the anterior distal femur has been considered as the reason for the observed bone loss. [6, 95, 96].

Also, during normal gait, load is transferred through the knee joint. Knee implant transfers the majority of this load (stress bypass). As a result, the proximal tibial bone is stress-shielded by tibial stem, and therefore, this will lead to bone resorption in the proximal tibia [20].

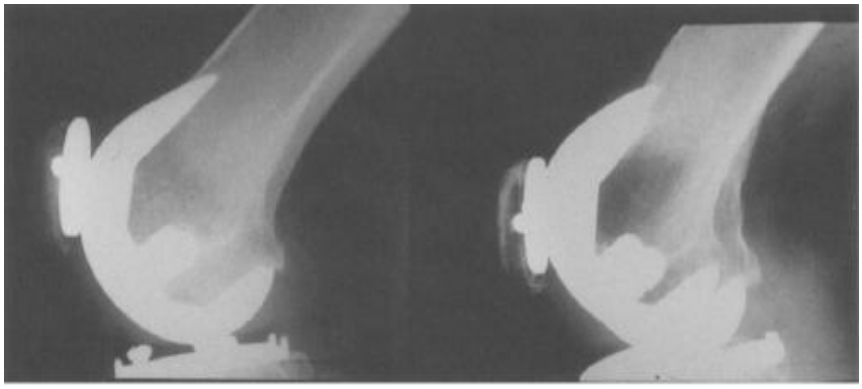

Fig. 1.16: Bone loss due to stress shielding; Left, immediately after uncemented TKA, Right, 4 years later [9].

Van Lenthe *et al.* [17] proved that insufficient bone stock which is noted frequently in revision surgery of femoral components of total knee arthroplasty can be created by stress shielding. They examined the similarity of clinical findings and the results of 3D finite element analysis of their model and showed that the stress shielding can induce distal femoral bone loss. Also, unlike the clinical findings they proved that bone resorption is a continuing process and the consequences of that can be a large amount of bone loss thereby needing large reconstruction at the time of revision surgery. Angelides *et al.* [18] examined the effect of the femoral component on the stress field in the distal femur and obtained the magnitude and direction of the three principal stresses. They realized that although the stress distribution in regions nearer to the prosthesis

remains similar after TKA, the stresses in the farther regions are reduced drastically. Au *et al*. [97] investigated the role of the loading conditions at the tibiofemoral joint interface and material properties of implant on the stress shielding (or bone stress state). They concluded the bone stress is reduced in presence of an implant with high-modulus material. Also, the tibiofemoral loading condition which includes loading pattern, load placement on the condylar surface, and bone or implant condylar surface geometry, can induce stress shielding by altering the stress distribution within the bone. For example, altering the geometry can cause 50% of the stress shielding. Sathappan *et al.* [20] conducted investigation on effect of utilization of the long-stem prosthesis on stress shielding in proximal tibia. Long-stem is intended to increase the interface area between bone and implant, therefore to increase the stability between them. Their results showed there was no significant change of bone mineral density or stress shielding in tibia using long-stem prosthesis. Huiskes *et al.* [12] investigated the relationship between implant flexibility and the magnitude of bone loss. The result was consistent with the hypothesis that bone resorption process is a respond of bone to the stress shielding. While stress shielding is decreased by using flexible stems, proximal interface stresses will be increased by them. Therefore, a method in which optimal characteristics of stem had been considered was proposed. During this investigation a *strain-adaptive* bone remodeling along with finite element models were used to simulate the bone remodeling process.

There are several bone remodeling theories that predict the bone behaviour in the presence of different stimuli. Since this study is intended to focus on theories that examine the adaptive remodeling process, chapters 3 and 4 will discuss such theories.

As this study includes biology and engineering subjects, the reviewed literature has been brought under relevant chapters for the convenience of the reader. *Chapter 2* lays out the research question, the aims and scope of this investigation. *Chapter 3* presents a review of some previous bone remodeling studies and theories. *Chapter 4* introduces the new model of bone remodeling, the thermodynamic-based theory, which is the basis of this study. *Chapter 5* presents the geometry modelling implemented in FEA. In *Chapter 6* a three-dimensional finite element (FE) model is developed using the software (ANSYS 12; ANSYS, Toronto, CA) to validate the thermodynamic-based theory of bone remodeling. *Chapter 7* includes the results and discussion and, finally, *Chapter 8* contains the conclusion, limitation, and proposed future work.

CHAPTER 2 CURRENT STUDY

In this investigation a new adaptive Thermodynamic-based bone remodeling theory proposed by Bougherara *et al.*, is implemented to predict the bone density distribution in the distal femoral bone before and after total knee arthroplasty. The results are then compared with the classical adaptive bone remodeling theory, i.e. Strain Energy Density (SED) theory as well as the clinical observations.

2.1 Problem statement

Currently, bone remodeling after total knee or hip arthroplasty is not accurately predicted. Yet a large number of bone remodeling models are based on continuum mechanics and neglect the interactions between bone and its surroundings. To accurately predicted bone remodeling, a new thermodynamic-based model which takes into accounts both mechanical and metabolic (biological and chemical) factors is proposed for the prediction of bone loss in the distal femoral bone before and after total knee arthroplasty.

2.2 Research question

Does the proposed thermodynamic-based model predict more realistically the evolution of bone density in the femur before and after TKA and how does this model compare to the conventional strain energy density model and clinical data?

2.3 Aims of this study

The distinct goals of this study are to:

1. Summarize relevant literature on knee joint anatomy, knee joint biomechanics, knee replacement procedures, and knee implants.
2. Develop a computer-aided, realistic geometry of the bone-implant knee prosthesis system.
3. Implement the new proposed theory of bone remodeling, i.e. the thermodynamic-based theory, and the classical theory, i.e. SED, with 3D Finite Element models to predict bone density distribution in a real bone.

4. Compute, compare and evaluate the density distribution predicted by the thermodynamic-based model with the strain energy model and clinical observations.

CHAPTER 3 LITERATURE ON BONE REMODELING THEORIES

3.1 Bone modeling and remodeling

Bone, like skin, forms before birth but continually renews itself thereafter. Even after bones have reached their adult shapes and sizes, old bone is continually destroyed, and new bone tissue is formed in its place.

In 1990, Frost stated "The modeling process molds the growth to produce organized structures from the microscopic level up to the level of the entire animal" [98]. In other words, modeling is a process in which bone is prevented growth in some locations and activated for growth in others [99].

Remodeling is a process in which overall size or structure of bone is not altered. "Remodeling removes old tissue and replaces it with new tissue, and may or may not change the architecture or size of the bone" [99]. Therefore, modeling has an important role in developing the adult bone structure, whereas remodeling is a continual process throughout the life.

Bone remodeling is the ongoing replacement of old bone tissue by new bone tissue. Remodeling also removes worn and injured bone, replacing it with new bone tissue [31, 100]. Figure 3.1 displays the bone remodeling process. Osteoclasts are responsible for the resorption of bone tissue. A delicate balance exists between the actions of osteoclasts in removing minerals and collagen and of bone-making osteoblasts in depositing minerals and collagen. If too much mineral is deposited in the bone, the surplus bone tissue may form thick bumps, called *spurs*, on the bone that can interfere with movement at joints. An excessive loss of calcium or inadequate formation of new tissue weakens the bones, making them overly flexible or vulnerable to fracture [31].

Normal bone metabolism (e.g., growth in the young, bone remodeling in the adult, and repair of fractured bone) depends on several factors. These include (1) adequate minerals; (2) vitamins; (3) several hormones; (4) weight-bearing exercise (exercise that places stress on bones) [31].

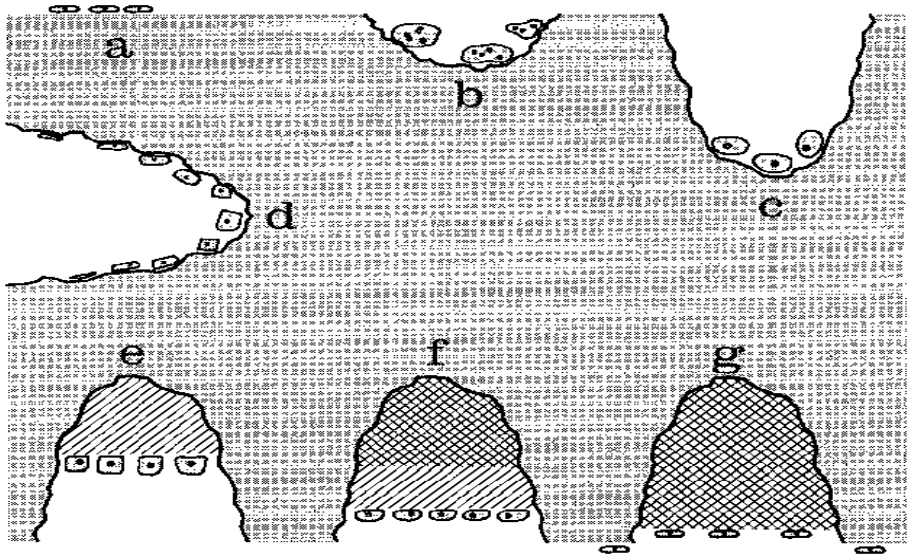

Fig. 3.1: "The remodeling cycle: (a) resting trabecular surface; (b) multinucleated osteoclasts dig a cavity of approximately 20 µm; (c) completion of resorption to 60 µm by mononuclear phagocytes; (d) recruitment of osteoblasts precursors to the base of the resorption cavity; (e) secretion of new matrix by osteoblasts; (f) continued secretion of matrix, with initiation of calcification; and (g) completion of mineralization of new matrix. Bone has returned to quiescent state, but a small deficit in bone mass persists" [100].

Within limits, bone tissue has the ability to alter its strength in response to mechanical stress. When placed under stress, bone tissue becomes stronger with time, through increased deposition of mineral salts and production of collagen fibers. Without mechanical stress, bone does not remodel normally because resorption outpaces bone formation. The absence of mechanical stress weakens bone through decreased numbers of collagen fibers and demineralization, loss of bone minerals. The main mechanical stresses on bone are those that result from the pull of skeletal muscles and the pull of gravity [31].

3.2 Literature review of bone remodeling theories

This section is intended to present some theories regarding bone remodeling not a comprehensive review of all theories.

In 1858, Humphrey [101] observed that trabeculae cross articular surfaces at right angles and proposed that forces are the major factors determining the shape and form of a bone.

In 1866, G.H. Meyer presented a paper on the structure of cancellous bone and demonstrated that "the spongiosa showed a well-motivated architecture which is closely connected with the statics and mechanics of bone" [102]. C. Culmann, a mathematician who had published a book on graphic statics in the same year, remarked that the lines in Meyer's drawings resembled the principal stress trajectories in cantilever beam. Meyer, in his paper published the following year (1867), stated that Culmann, stimulated by the drawings of bone structure, asked a student of his to construct the principal stress trajectories in a crane-like curved bar loaded in a fashion similar to the human femur. Meyer formulated his ideas in three questions:

1) Is it possible that structures like the observed ones are formed by static (force-equilibrium) conditions?
2) What is the internal metamorphosis that makes these structures so "fit for service"?
3) Can these structures be understood if one adds to the external loads the mechanical influence of the traction of muscles and ligaments?

Two years later, Wolff realized that Culmann's crane structure was precisely consistent with the trabecular structure of the human femur [99] and claimed:

1) There is a perfect mathematical correspondence between the structure of cancellous bone in the proximal end of the femur and the trajectories in Culmann's crane.
2) There is a statical importance and necessity of the trajectorial structure of the bone.
3) Bone growth can occur only in the interstitial space.
4) The compact bone is nothing but a compressed cancellous bone [102].

Wolff developed his ideas and published his famous work, *The Law of Bone Remodeling*, in 1892 [99].

Wolff's theory was summarized by Treharne [103] as: "Every change in the … function of a bone … is followed by certain definite changes in … internal architecture and external conformation in accordance with mathematical laws".

The concept of bone adaptation has been considered as the basic of developing subsequent researches and bone remodeling theories by most researchers.

As previously mentioned, Bougherara *et al.* [21] classified the mathematical theories explained the relationship between mechanical forces and bone structure into three groups: (1) Mechanical; (2) Mechanobiological; (3) Biochemical.

In mechanical theories, most researchers assumed that bone density distributions are optimized with respect to magnitude of the local stress, meaning, areas exposed to higher stresses have higher cortical thicknesses. Therefore, the net rate of remodeling is related to magnitude of the mechanical stimulation, namely stress, strain or strain energy density [98]. Some researchers develop bone remodeling theories in terms of bone strains rather than stresses, because it has a physical sense and represents a measurable displacement of two material points [104-106].

Cowin *et al.* proposed a dynamic theory of cortical bone remodeling in 1976. In this theory, an elastic relation for cancellous bone with a combination of the stress and strain tensors was developed. The principal axes of strain and stress coincided at remodeling equilibrium [107,108].

In 1984, Cowin's theory was used to develop a 3D finite element model by Hart *et al.* [109]. This model was able to change geometry and material properties according to local strain, thereby updating in time steps to provide incremental remodeling predictions. But, they could not use the model in existing experimental studies to predict results, because, they had to estimate the surface remodeling rate by trying to obtain the pre-existing results [25].

In 1986, Fyhrie and Carter [110] proposed a theory in which the orientation and structure of trabecular bone coincides with a minimized strain energy criterion. They also used an effective energy stress to predict apparent density.

Some researchers have divided the mechanical remodeling theories into two categories; (1) time-dependent and (2) time-independent. In the application of these theories, the remodeling process usually is divided into internal and external (or surface) remodeling. In the internal remodeling, the geometry of the model is bonded and the distribution of material properties changes with time [111-113]. In 1989, Hart and Davy [114] computationally simulated internal and external remodeling. They assumed a cylindrical geometry and therefore their equations for internal remodeling only apply to remodeling in cortical bone [25].

As one can see in foregoing developments, mechanical models are based on Wolff's Law and it is assumed that bone density changes in a time rate to respond the mechanical stimulus. According to Huiskes *et al.* [11], these theories have three major defects: (1) they relates stress or strain in bone to adaptive remodeling behaviour, without considering biological mechanisms; (2) theories of linear elasticity are assumed valid for the bone material; (3) effects of loading rates, visco-elastic and inertial effects are not considered. Huiskes *et al.* proposed their famous strain energy density theory of adaptive bone remodeling in 1987. Later on, the SED theory was expanded by Weinans *et al.* [22]. Since this theory is known as the classical adaptive bone remodeling model, the thermodynamic-based theory of bone remodeling will be compared with it as a part of the Results chapter of this thesis. Therefore, the SED theory will be discussed in details in the following section.

In mechanobiological theories, mechanical forces along with osteoblasts and osteoclasts activities have important roles to predict bone remodeling behaviour. The base of these theories originates from Roux who considered bone as a self-organize tissue [5].

In 1987, Frost [115] developed his famous 'mechanostat' theory to predict bone adaptation behaviour based on mechanical and biological stimuli. In his bone remodeling theory, a fundamental assumption is made that the bone adaptation process is error driven; that is, the magnitude of the response is based on the difference between the local strain state due to the applied mechanical load and a biological set point. Loads well below the set point stimulate bone removal and subsequent reductions in local bone stiffness. Reduced local stiffness leads in turn to increases in local strains until the set point is reached (or approximated) and the bone is adapted to the loading stimulus.

Huiskes *et al.* [24] presented a computational model showing feedback from mechanical load transfer, balance bone mass in a coupled homeostatic process of remodeling. In 2000, Hernandez *et al.* [116] proposed a model describing influence of biologic factors on osteoblasts and osteoclasts. The primary accomplishment made in their model was that the mechanobiologic response changes osteoclasts and osteoblasts activities instead of just causing net resorption. Therefore, it made a more detailed description of remodeling and showed the relationship between mechanobiologic and metabolic responses through their effects on osteoblasts and

osteoclasts. They also described bone adaptation to metabolic factors including nutrition, drugs, and disease.

In biochemical theories, the activity of osteoclasts and osteoblasts is examined to obtain insight into the bone remodeling process considering metabolic factors. Several models have been proposed based on this theory. Earlier works described the role of Parathyroid Hormone (PTH) as a regulator in bone remodeling process [117,118]. PTH acts on both bone resorbing cells and bone forming cells, but has differing effects depending on whether it is administered continuously or not. When administered continuously, it increases Osteoclastic bone resorption and suppress bone formation. However, when administered in low doses intermittently, it stimulates bone formation without major effects on resorption, a response that has been referred to as the so-called *anabolic* response to PTH [119]. Later, the roles of other hormones were examined. For example, in [120,121] it has been described that the advancement of bone remodeling is conducted by numerous autocrine and paracrine factors. Mundy *et al.* in 1987 stated "Osteoclastic resorption may be stimulated by factors that enhance proliferation of osteoclast progenitors, which cause differentiation of committed precursors into mature cells or activation of the mature multinucleated cell to resorb bone" [122]. Although these theories consider metabolic factors to give insight into bone remodeling process, not considering role of mechanical stimulus in the process is their significant defect.

In 2010, Bougherara *et al.* [21] proposed a novel bone remodeling theory based on nonequilibrium thermodynamics principles considering both mechanical and metabolic (chemical and biological) factors as driving factors in bone remodeling. As the purpose of current study is based on the thermodynamic-based bone remodeling theory, this theory is discussed in detail in the following chapter.

3.3 Strain Energy Density (SED) theory of bone remodeling

The strain energy density (SED) model of bone remodeling was developed by Huiskes *et al.* in 1987 [11]. This model uses (strain energy) / (bone volume) or U as the mechanical signal that advances and controls the bone remodeling process. The strain energy density U can be expressed in terms of stresses and strains as follows [123]:

$$U = \frac{1}{2}\sigma_{ij}\varepsilon_{ij} \tag{3.1}$$

Since, according to the internal bone remodeling theory, the SED and the rate of change of bone density have a linear relationship, the remodeling governing equation can be written as follows:

$$\frac{d\rho}{dt} = B\left(\frac{U}{\rho} - k\right), 0 < \rho \leq \rho_{cb} \tag{3.2}$$

where ρ is the apparent density of the bone, ρ_{cb} represents the maximum density of the cortical bone, the constants B and k are the remodeling rate and the site-specific reference SED, respectively.

According to Carter *et al.* [124], the difference between the actual strain energy density and a reference (target) one (*k*) is the driving force for remodeling process. In fact, it is assumed that there is a threshold level "s" which must be exceeded before bone remodeling could be initiated. This threshold is called *dead zone*, and its value correspond to $\left(s \pm 1 = U/\rho/k\right)$ (Fig. 3.2).

Considering Fig. 3.2 and the value of threshold "s", the governing differential equation of the adaptive bone remodeling process (Eq. 3.2), can be restated as follows:

$$\frac{d\rho}{dt} = \begin{cases} B\left[\dfrac{U}{\rho} - (1-s)k\right], & \text{if } \dfrac{U}{\rho} < (1-s)k \quad \text{resorption,} \\ 0, \text{ if } (1-s)k \leq \dfrac{U}{\rho} \leq (1+s)k \quad \text{dead zone,} \\ B\left[\dfrac{U}{\rho} - (1+s)k\right], & \text{if } \dfrac{U}{\rho} > (1+s)k, \text{ formation} \end{cases} \tag{3.3}$$

The change in bone density in each iteration is obtained by solving the step Eq. 3.3 and can be expressed as follow [123]:

$$\begin{aligned} &\Delta\rho(x,t) = \Delta t.B\left(\frac{U}{\rho} - k(1 \pm s)\right) \\ &0 < \rho \leq \rho_{cb} \end{aligned} \tag{3.4}$$

Considering Eq. 3.4, the new bone is obtained simply by the following equation:

$$\rho(x, t+\Delta t) = \rho(x,t) + \Delta\rho(x,t) \tag{3.5}$$

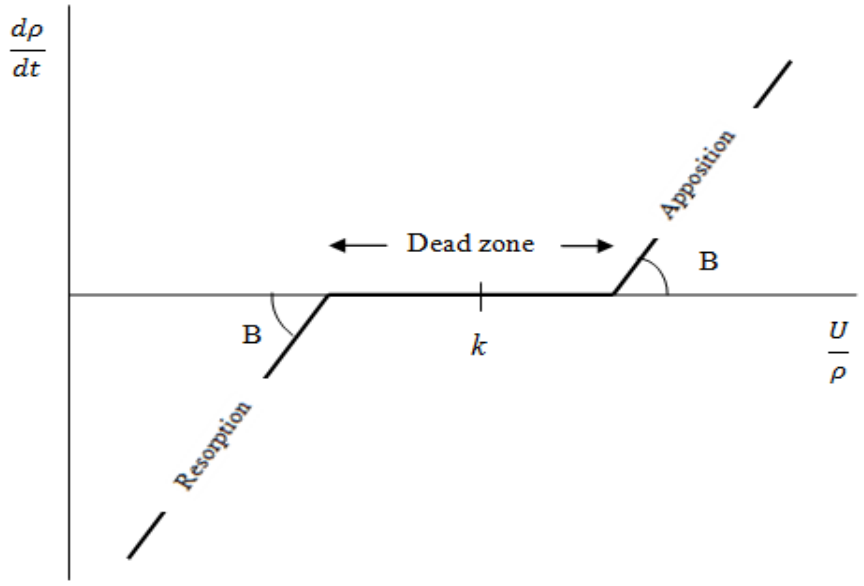

Fig. 3.2: SED theory of bone remodeling process as proposed by Huiskes et al. [123].

This iterative process will stop if no significant changes in bone density in any element and in any step are observed. Mathematically speaking,

$$CONVD = \frac{1}{n}\sum_{i=1}^{n}\left|\left(\rho_i^{(t)} - \rho_i^{(t-1)}\right)\right| \tag{3.6}$$

where "*n*" is the number of elements in the FE model, "*i*" is the element index, and CONVD is the sum of the absolute values of variation in relative apparent density. If the value of CONVD reaches an amount of 0.01, which means the change in bone density is almost zero in all elements, the bone remodeling process ends and equilibrium is reached. The boundary condition for the predicted apparent density is given by the following relation:

$$\rho_{\min} \leq \rho \leq \rho_{cb} \tag{3.7}$$

There are different relationships between density and elastic modulus in the literature to calculate the elastic modulus of the bone after each iteration. Bougherara *et al.* used the one proposed by Keller in which the bone density (g/cm^3) is correlated to the elastic modulus (GPa) as follows [123]:

$$E = 10.5\rho^{2.57} \tag{3.8}$$

It should be noted Weinnans *et al*. [125] showed that the FE models provide consistent stress-shielding patterns in the bone, independent of the choice of the bone density modulus relationship used in the computer model.

According to Bougherara *et al.* [123] the parameter values presented in Table 3.1 lead to reasonable bone configuration. Therefore, for the numerical simulation of the distal femoral bone using strain energy density (SED) model discussed in Chapter 7 these values are considered.

Table 3.1: Values of parameters in strain energy density model used by Bougherara *et al*. [123].

Parameter	Unit	Value
B	$(g/cm^3)^2$ / MPa × time unit	1
k	J/g	0.004
E	MPa	$10500\rho^{2.57}$
s	-	0.35
ρ_{min}	g/cm^3	0.01
ρ_{max}	g/cm^3	1.74

CHAPTER 4 IRREVERSIBLE THERMODYNAMIC-BASED THEORY

4.1 Introduction

Irreversible thermodynamics is the branch of physical sciences capable of explaining the spontaneous generation and propagation of natural order.

An irreversible (non-equilibrium) process is one in which there occurs irreversible changes in the system or in the surroundings or in both. The irreversible changes take place due to rapid dissipation of energy. During non-equilibrium process the entropy of the system and the surrounding increases. For example, when a match-stick is struck to cross the activation energy barrier the chemicals are ignited and burn rapidly to take the system and the surroundings to a state of maximum entropy by formation of gaseous and the liberation of heat. In such reactions both physical and chemical changes occur which cannot be reversed. Non-equilibrium thermodynamics make it possible for the occurrence of biological reactions in open system. Such processes are forbidden in closed systems and therefore, the presence of open systems mechanics is of paramount importance in the creation and sustenance of living matter [102].

Bougherara *et al.* proposed the thermodynamic-based theory of bone remodeling in 2010. According to this theory, there is a relationship between the dynamic loading and chemical reaction which induces change in bone tissue density based on irreversible thermodynamics principles. In this chapter, this theory is reviewed in detail.

4.2 The laws of thermodynamics

Classical thermodynamics is based on the following rules:

1) Conservation of matter,
2) An isolated system tends toward equilibrium,
3) The first law: conservation of energy,
4) The second law,
5) The third law [126].

4.2.1 The first law

Davy and Joule showed that if a small amount of heat dQ is imparted on a body, the body would change its state and do work:

$$d\mathcal{U} = dQ - dW \tag{4.1}$$

The variable $\mathcal{U}$ is a function of the state of the body; W is the work done by the system on the surrounding. Equation (4.1) is a statement of the *first law of thermodynamics*. Then according to the law of conservation of energy the energy gained by the system is equal to the energy lost by the surrounding. As the energy $\mathcal{U}$ is a state function, the energy change depends upon the initial and final states of the system and not on the manner in which the change takes place [102].

Joule and others, in establishing the first law, experimented on many forms of work and energy: mechanical, electrical, chemical, etc. If the body is a solid and the stress in the body is σ_{jk} and the body deforms so that its strain is changed by de_{jk}, then the work done by the stress is $\sigma_{jk}\, de_{jk}$ per unit volume, or $\sigma_{jk}\, de_{jk}V$ in a body of volume V. If a force $\mathbf{F}$ acts on a material particle which is moved by a displacement $\mathbf{dx}$, then the work done is $\mathbf{F}.\mathbf{dx}$. If a muscle shortens by an amount $-\mathbf{dL}$ under a force $\mathbf{\mathcal{F}}$, it performs work equal to $-\mathbf{\mathcal{F}}.\mathbf{dL}$. If a quantity of electricity $-de$ is given off by a system at an electric potential ψ, an electric work ψde is performed. If dn_i mole of the ith species of chemicals is transported into the system from the surrounding, a chemical energy $\mu_i dn_i$ is added to the system (the constant of proportionality μ_i is called the *chemical potential*). Thus, on denoting the change of energy by $d\mathcal{U}$ for a solid body containing muscle fibers and subject to a body force $\mathbf{F}$, an electric potential ψ, and a transfer of N species of chemicals No. 1, 2, …, N into the body by the amounts dn_1, dn_2, …, dn_N, we have, by the first law:

$$d\mathcal{U} = dQ + \mu_\alpha dn_\alpha - \boldsymbol{\mathcal{F}}.\mathbf{dL} + \mathbf{F}.\mathbf{dx} - \psi de + \sigma_{jk}\, de_{jk}V. \tag{4.2}$$

The Greek index α ranges over 1, 2… N. The summation over α includes all chemical species of the system. The energy $d\mathcal{U}$ includes kinetic, potential, and internal energies [126].

4.2.2 The second law

The *second law of thermodynamics* may be stated as follows:

There are existing two single-valued functions of state T, called the absolute temperature, and S, called the entropy, with the following properties:

I. T is a positive number which is a function of empirical temperature only.

II. The entropy of the system is equal to the sum of the entropies of its parts.

III. The entropy of a system can change in two distinct ways: by transfer from the surrounding and by internal changes. Thus

$$dS/dt = dS_i/dt + dS_e/dt \tag{4.3}$$

where dS/dt denotes the rate of increase of entropy of the system, d_eS/dt denotes the rate of transfer of entropy from the surrounding, d_iS/dt denotes the rate of change in entropy taking place within the system.

IV. The internal entropy production, the amount of entropy created per unit time d_iS/dt, is never negative, because an isolated system cannot spontaneously create an order in itself. Thus a physical process resulting in a negative d_iS is not realizable in nature even if the process may conserve energy. However, a process by exchanging energy and matter with the surrounding will have positive or negative d_eS. If d_iS is zero, the process is said to be reversible. If it is positive, the process is said to be irreversible. Therefore the fundamental quantity which tells us whether a process is reversible or irreversible is d_iS/dt.

V. If dQ is the heat absorbed by a system in a reversible process, then the entropy of the system is changed by the amount:

$$dS = \frac{dQ}{T} \tag{4.4}$$

The absolute temperature T and the entropy S are defined completely by their properties as expressed in the second law. Combining equations (4.2) and (4.4),the first and second laws, we obtain the *Gibbs equation* for a tissue containing muscle fibber with tension **F**, subject to external force **F**, electric potential ψ, and transfer of **N** species of chemicals of mass dn_1, dn_2… dn_N into the tissue [102, 126],

$$d\mathcal{U} = TdS + \mu_\alpha dn_\alpha - \boldsymbol{F}.\boldsymbol{dL} + \boldsymbol{F}.\boldsymbol{dx} - \psi de + \sigma_{jk}\, de_{jk} V \tag{4.5}$$

According to the second Law of Thermodynamics a dissipative or irreversible process taking place in the system will cause an increase in the entropy of the system.

If *Gibbs equation* is written in a form that refers to intensive, or local, variables only, we will have:

$$Tds = du + pdv - \Sigma \mu_i dw_i \qquad (4.6)$$

where *s, u, v*, and w_i stand for the specific values of the entropy, energy, volume, and mass of the substance i; that is, if 'm' is the total mass of the subsystem containing the point considered, then $s = S/m$, $u = U/m$, $v = V/m$, and $w_i = m_i/m$ (the mass fraction of substance *i*) [127].

4.2.3 The third law

The second law states how entropy of a system is changed, but it does not say how an absolute value can be assigned to entropy. The assignment of an absolute value of entropy is done by the *third law of thermodynamics: The entropy in the state T = 0 is equal to zero in every system occurring in nature.*

4.3 Onsager Reciprocal relation

In an irreversible process, there is a flow of heat, mass and electric charge etc. It is the *driving force* which produces the flow. The driving force is usually described by the gradient in some physical properties. A temperature gradient is the driving force for the flow of heat. Concentration gradient is the driving force for the transfer of mass and electric potential acts as the driving force for the current in the flow of electric charge. The flow of any quantity such as heat or mass or electric current per unit area, called the *flux*, is then postulated to be proportional to the driving forces and an analytical expression is formulated:

$$J_Q = -K_t \frac{\partial T}{\partial x} \qquad (Fourier's\ Law) \qquad (4.7)$$

$$J_m = -D \frac{\partial C}{\partial x} \qquad (Fick's\ Law) \qquad (4.8)$$

$$J_e = -K_e \frac{\partial E}{\partial x} \qquad (Ohm's\ Law) \qquad (4.9)$$

where J is the flux [127].

The proportionality constants K_t, D and K_e are called the thermal conductivity, mass diffusion coefficient and electric conductivity. If only one driving force (gradient) is present in a system, we say that there is *single flow* associated with the gradient of the property. The process can then be described by some type of phenomenological relation. If more than one driving force is

present in the system, there will be more than one flow. When more than one flux is present in the system, we say that these are *coupled flows*. Each flux J_i is assumed to be related to each gradient or driving force X_i by the following *linear* relation [102]:

$$J_i = L_{i1}X_1 + L_{i2}X_2 + L_{i3}X_3 + \ldots \tag{4.10}$$

Thus for flux 1, we have:

$$J_1 = L_{11}X_1 + L_{12}X_2 + L_{13}X_3 + \ldots \tag{4.11}$$

and for flux 2, we write:

$$J_2 = L_{21}X_1 + L_{22}X_2 + L_{23}X_3 + \ldots \tag{4.12}$$

and so on. The resulting equations like (4.11) and (4.12) etc. are called the linear *phenomenological equations*; and the coefficients L_{ij} are called *Onsager phenomenological coefficients*. The above equation is not free from complications because the coefficients L_{ij} must be determined experimentally. Experimental determination of the coupling coefficients can be a tedious matter, as it involves large number of parameters which must be kept under strict control. An analytical relationship is devised to overcome this difficulty [102]. This device is the Onsager Reciprocity Relation,

$$L_{ij} = L_{ji} \tag{4.13}$$

This relation applies to systems in the absence of a magnetic field. The utility of this equation can be exemplified. Assuming two fluxes and two driven forces, we will have from Eq. (4.10):

$$J_1 = L_{11}X_1 + L_{12}X_2 \tag{4.14}$$

$$J_2 = L_{21}X_1 + L_{22}X_2 \tag{4.15}$$

Given X_1 and X_2, knowledge of four coefficients is necessary to determine the two fluxes J_1 and J_2. Now when the Reciprocity Relation is used, we have $L_{12} = L_{21}$, and only three coefficients are necessary; namely, L_{12}, L_{11} and L_{22}. The latter two coefficients are the primary coefficients which are usually readily available [102].

4.4 Chemical reactions of bone remodeling

The bone remodeling process is based on the activities of bone resorbing cells known as osteoclasts and bone forming cells known as osteoblasts. According to Bougherara *et al.* [21] bone remodeling can be considered as a process with three different stages: (1) bone resorption,

(2) bone formation, (3) growth control. It is focused just on bone resorption and formation in the thermodynamic based theory of remodeling.

Five chemical reactions (ρ = 1-5) have been considered for bone remodeling process. All these reactions have the general form of the irreversible Michaelis-Menten scheme,

$$E + S \underset{k_{-1}}{\overset{k_{+1}}{\rightleftarrows}} C \overset{k_2}{\rightarrow} E + P$$

where E, S, C and P display enzyme, substrate, complex and product respectively [128].

The five reactions are as follow [21]:

$$R_1 + MCELL \underset{k_{-1}}{\overset{k_{+1}}{\rightleftarrows}} MNOC + R_4 \qquad \rho = 1$$

where R_1 is mixture of all substances that are initiating the reaction with mononuclear cells (MCELL). MNOC depicts the multinucleated osteoclasts and R_4 is the remaining product. The next reaction depicts how to be dug a cavity by multinucleated osteoclasts.

$$MNOC + Old\_B \underset{k_{-2}}{\overset{k_{+2}}{\rightleftarrows}} R_6 + R_7 \qquad \rho = 2$$

where Old_B is the abbreviation for old bone, and R_6 and R_7 are production of bone decomposition. According to a biological rule, chemical reactions in nature are well optimized meaning products resulting from bone decomposition (R_7) participate in the activation of osteoblasts. Therefore,

$$R_7 + Old\_B \underset{k_{-3}}{\overset{k_{+3}}{\rightleftarrows}} Activ\_OB + R_9 \qquad \rho = 3$$

The activator Activ_OB produced by this reaction activates osteoblasts (OB) to fill the eroded cavities produced by osteoclasts activities as following reaction:

$$Activ\_OB + OB \underset{k_{-4}}{\overset{k_{+4}}{\rightleftarrows}} Osteoid + R_{12} \qquad \rho = 4$$

The last stage is bone calcification and completion of mineralization of new matrix:

$$R_{13} + Osteoid \underset{k_{-5}}{\overset{k_{+5}}{\rightleftarrows}} New\_B + R_{15} \qquad \rho = 5$$

where R_{13} is the substance which initiates the mineralization process, New_B is the new bone formed by remodeling process and R_{15} is the remaining of bone formation process. According to Bougherara *et al.* [21], two stage of resorption and formation of bone remodeling process are described by foregoing five equations ($\rho = 1 - 5$).

4.5 Bone remodeling description based on thermodynamics principles

According to Bougherara *et al.* [21], bone remodeling process can be considered as a process that occurs in an open irreversible thermodynamic system. As bone remodeling includes two processes of bone resorption and formation, it is called a *coupled process*.

As described in section 4.2 and subsequent sections, the *Gibbs equation* (i.e., Eq. 4.5) can be written as follow:

$$d\mho = Tdy + \mu dN - pdV + \phi dq + etc. \qquad (4.16)$$

where y is called the *entropy source density* which is the *entropy production per unit volume*; *pdV*, *μdN*, and *ϕdq* are mechanical, chemical and electrical contributions respectively. According to [21], it is assumed that bone remodeling is mainly continued by the interaction between the mechanical and chemical fluxes or forces. Also, as described in subsection 4.2.2, the entropy production cannot be negative and is represented by integrating of Eq. (4.16). Thus:

$$Ty(S) = pd_{(1)} + \omega_\rho A_\rho \qquad (4.17)$$

where $d_{(1)}$ is the rate of deformation tensor, p is a pressure or mechanical energy concentration, ω_ρ and A_ρ are the *chemical reaction rate* and *affinity* of ρth reaction, respectively. The affinity for ρ_i is defined by:

$$A_\rho = - \Sigma_j \mu_j . \upsilon_{j\rho}$$

where the stochiometric coefficient $\upsilon_{j\rho}$ represents the number of molecules formed ($\upsilon_{j\rho}>0$) or destroyed ($\upsilon_{j\rho}<0$) by the chemical reaction ρ [129].

Since bone remodeling is considered as a coupled process between bone resorption and formation, and as described in section 4.3, the Onsager's relation expressing the cross-coupling between the pressure p and chemical reactions rates ω_ρ is as follow:

$$p = l_{vv} d_{(1)} + l_{v\rho} A_\rho \tag{4.18}$$

$$\omega_\rho = l_{\rho v} d_{(1)} + l_{\rho\rho} A_\rho \tag{4.19}$$

where l_{vv} is called *direct coefficient related to the viscosity* and $l_{\rho\rho}$ is called *direct coefficient related to the chemical reaction rates*. Also, according to section 4.3, $l_{v\rho}$ and $l_{\rho v}$ are the *cross coefficients* resulting from the coupling which must satisfy the Onsager's reciprocal relation ($l_{v\rho} = l_{\rho v}$) and the second law of thermodynamics. According to [21], if Eqs. 4.18 and 4.19 are substituted in Eq. 4.17, the Onsager's reciprocal relation and the second law of thermodynamics will be satisfied under the following constraints:

$$l_{vv} > 0 \text{ and } l_{\rho\rho} > 0 \text{ and } \quad q = \frac{l_{v\rho}}{\sqrt{l_{vv} l_{\rho\rho}}} \in (-1,1) \tag{4.20}$$

where q is the coupling parameter.

4.6 The role of mechanical loading and chemical reaction in bone remodeling

According to Bougherara *et al.* [21], the efficiency of the transformation of chemical energy into mechanical activity is described by following equation:

$$H = \frac{\omega_\rho A_\rho}{p d_{(1)} + \omega_\rho A_\rho} \tag{4.21}$$

where H is the efficiency of interaction.

To clarify the role of mechanical loading in remodeling, the ratio of $d_{(1)}$ and A_ρ was denoted as:

$$\delta = \sqrt{\frac{l_{\rho\rho}}{l_{vv}}} \frac{d_{(1)}}{A_\rho} \tag{4.22}$$

Combining Eqs. 4.20, 4.21, and 4.22:

$$H = \frac{\delta q + \delta^2}{1 + 2\delta q + \delta^2} \tag{4.23}$$

The sign of ω_ρ is estimated by the quantity H. The denominator of Eq. 4.21 is always positive, according to Eq. 4.17 and the second law of thermodynamic; therefore the sign of H is

correspond to the sign of $\omega_\rho A_\rho$. As in nature all systems, including living tissues, are well optimized, it can be assumed that the efficiency H has the absolute maximum value and it obtains by following relation [21]:

$$H_{max} = 1 \pm \frac{1}{2} \frac{q^2}{\sqrt{1-q^2}(1 \pm \sqrt{1-q^2})} \quad (4.24)$$

Thus the real effect of chemical reaction is Eq. 4.24.

According to Bougherara *et al.* [21], the driving force for all chemical reactions described by equations ρ = 1-5 are affinities A_ρ. The sign of A_ρ can be positive or negative depending on the values of chemical potential of products and substrates. If the chemical potential of product μ_p is greater than chemical potential of substrate μ_s, the affinity A_ρ is positive and the chemical reaction proceeds in the direction $S \rightarrow P$ and its rate is positive ($\omega_\rho > 0$). In case of $\mu_p - \mu_s \leq 0$ ($A_\rho < 0$), the corresponding chemical reaction cannot proceed spontaneously and a positive rate $\omega_\rho > 0$, which physiological remodeling corresponds to it, is guaranteed only by mechanical loading $l_{\rho v} d_{(1)}$ (Eq. 4.19).

4.7 Kinetics of chemical reaction

The *rate of reaction* is defined as the ratio of decreasing in concentration of reactants to time in which the change takes place. Also, the rate of reaction can be defined as the ratio of increasing in concentration of products to time in which the change takes place.

Likewise, the general form of the *rate equation* which has been obtained experimentally involving a reaction between A and B is:

$$\text{Rate} = k [A]^a [B]^b \quad (4.25)$$

This equation shows relation between the rate of reaction and the concentrations of reactants A and B where ‘k’ is the rate constant, ‘a’ and ‘b’ are the order of reaction with respect to A and B, and [A] and [B] are the concentration of reactants A and B, respectively [130].

Considering definition of the rate of reaction and Eq. (4.25) and also the fact that bone acts as an open self-organizing system that changes matter, energy and entropy, the change of the concentration of reactants in the point ‘x’ and time t is as follow [21]:

$$\frac{d[n]}{dt} = \dot{n}_i = \sum_{\rho=1}^{5} (v'_{\rho i} - v_{\rho i})\, \omega_\rho \tag{4.26}$$

where i = 1, 2, …, 15 and indicates the chemical reactants MCELL, MNOC, …, R_7, …, R_{15}, $v_{\rho i}$ is the stoichiometrical coefficient of *i*th chemical component for substrates and $v'_{\rho i}$ is the stoichiometrical coefficient of *i*th chemical component of products. After solving the kinetic chemical equations of 5 substances (Appendix), the concentrations of MCELL, Old_B, Activ_B, Osteoid, and New_B obtained are as follow [21]:

$$N_{MCELL} = 0.5\left(-\beta_1 + \sqrt{\beta_1^{\,2} + 4\frac{-D_1 + J_3 + J_{14}}{\delta_1}}\right) \tag{4.27}$$

$$N_{Old\_B} = 0.5\left(-(\beta_7 + 2\beta_3 - 2N_{MCELL}) + \sqrt{(\beta_7 + 2\beta_3 - 2N_{MCELL})^2 + 4\left(\frac{J_{14} - D_3}{\delta_3} + 2(J_{14} - D_2)\right)}\right) \tag{4.28}$$

$$N_{Activ\_OB} = 0.5\left(\begin{array}{l} -(\beta_{10} + 0.5\left(N_{Old\_B} - \beta_7 + \dfrac{J_{14} - D_3}{\delta_3 N_{Old\_B}}\right)) + \\ \sqrt{(\beta_{10} + 0.5\left(N_{Old\_B} - \beta_7 + \dfrac{J_{14} - D_3}{\delta_3 N_{Old\_B}}\right))^2 + 4\dfrac{J_{14} - D_4}{\delta_4}} \end{array}\right) \tag{4.29}$$

$$N_{Osteoid} = 0.5\left(-(\beta_{13} - \beta_{10} + \frac{J_{14} - D_4}{\delta_4 N_{Activ\_OB}}) + \sqrt{(\beta_{13} - \beta_{10} + \frac{J_{14} - D_4}{\delta_4 N_{Activ\_OB}})^2 + 4\frac{J_{14} - D_5}{\delta_5}}\right) \tag{4.30}$$

$$N_{New\_B} = -N_{Osteoid} + \beta_{10} - \frac{J_{14} - D_4}{\delta_4 N_{Activ\_OB}} \tag{4.31}$$

where N_i is the rate of concentration of the *i*th substance, δ_ρ is the ratio of rate of ρth reaction to second reaction, D_ρ is the parameter that describes the influence of dynamical loading on rate of ρth chemical reaction, β_i is sum of corresponding initial concentrations and J_i are fluxes of substances. More details are presented in section 4.10.

4.8 Calculation of density and elastic modulus of the bone

In Chapter 6, the time evolution of old and new bone described by Eqs. (4.28) and (4.31) will be tested in a standard distal femur before and after TKA to qualitatively simulate bone adaptation induced by daily walking activity. For this purpose and according to Bougherara *et al.* [21], the density and elastic modulus in each element are obtained from the following equations:

$$\rho\,(I) = \rho_0(N_{Old\_B}(I) + N_{New\_B}(I)) \tag{4.32}$$

$$E(I) = \left(E_{Old}\left[\frac{N_{Old\_B}}{N_{Old\_B}+N_{New\_B}}\right] + E_{New}\left[\frac{N_{New\_B}}{N_{Old\_B}+N_{New\_B}}\right]\right)\left(\frac{\rho(I)}{\rho_0}\right)^3 \quad (4.33)$$

where ρ_0 is the initial density of the composite bone that is assumed to be equal to the average value of the density of cortical and cancellous bones and is used to obtain the material properties of the bone initially; after that the properties are changed by bone concentration of old and new bone [131]. It will be discussed more in subsection 6.2.1. E_{Old} is the elastic modulus of the composite bone before arthroplasty and E_{New} is the expected elastic modulus after surgery, which both are measurable and are given.

4.9 Dynamic loading

Bougherara *et al.* [21] assumed that there is a linear relationship exists between the influence of the strain rate on the ρth chemical reaction D_ρ and the rate of the deformation tensor $d_{(1)}$:

$$D_\rho(I) = C d_{(1)}(I) \quad (4.34)$$

As ANSYS calculates only the deformation (or the trace of the strain ($\in_{(1)}(I)$), sum of principal strains) and stresses in each element of bone, the rate of the deformation tensor $d_{(1)}$, strain rate, used in Eq. (4.34) can be obtained by:

$$d_{(1)}(I) = \frac{d\in_{(1)}(I)}{dt} \approx \frac{\Delta\in_{(1)}(I)}{\Delta t} \approx \frac{\in_{(1)}(I)}{\Delta t} \quad (4.35)$$

where Δt is the time of loading. Combining Eqs. (4.34) and (4.35):

$$D_\rho(I) = C\frac{\in_{(1)}(I)}{\Delta t} \quad (4.36)$$

where C is a constant which can be obtained by :

$$C = \frac{D_\rho(ref)}{S(ref)} \quad (4.37)$$

where $D_\rho(ref)$ is the influence of the reference strain rate on the ρth chemical reaction and $S(ref)$ is the reference strain rate. In this study the reference values used in FEA are considered similar those in [21] as shown in Table 4.1.The combination of Eqs. (4.36) and (4.37) leads to:

$$D_\rho(I) = \frac{|d_{(1)}(I)|}{S(ref)} D_\rho(ref) = \frac{1}{\Delta t}\frac{|\in_{(1)}(I)|}{S(ref)} D_\rho(ref) \quad (4.38)$$

The absolute value is used because the tensile load is followed by reduction and the compressive load is followed by an expansion.

4.10 Parameters of the proposed thermodynamic model used in the FE simulations

For the numerical simulation of the femoral model described in Chapter 6, Bougherara *et al* [21] used the values of constant parameters, applied in Eqs. 4.27-4.31, showed in Table 4.1. Utilizing these values, they found that bone density distributions using thermodynamic-based model is quite comparable with the classical adaptive bone remodeling model (Strain Energy Density) developed previously by Huiskes *et al* [24]. In this study, therefore, the same parameter values are utilized in Eqs. 4.27-4.31.

Table 4.1: Values of Parameters used in Eqs. 4.27-4.31 [21]

Parameter	Value	Parameter	Value
β_1	5.23	δ_4	5.75
β_3	16.5	δ_5	3.08
β_7	4.08	D_1(ref)	2.44
β_{10}	2.28	D_2(ref)	1.26
β_{13}	4	D_3(ref)	5.85
J_3	2.38	D_4(ref)	1.3
J_{14}	5.07	D_5(ref)	4.68
δ_1	20.29	S(ref)	3*3500E-6
δ_3	10.03		

CHAPTER 5 GEOMETRY MODELLING

5.1 CAD model of the femur

The synthetic “fourth generation femur” model was scanned by computed tomography (CT). CT is a non-destructive imaging technique, using X-ray beams, for producing 2D and 3D cross sectional of an object. A series of 2D cross sectional images at intervals of 0.5 mm along the length of the femur across the three planes of the body (coronal, sagittal, and axial) were taken. Then CT images were imported into MIMICS Medical Imaging Software (The Materialise Group, Leuven, Belgium), for visualization and production of 3D images. The 3D model included geometry data for both cortical (outer layer) and cancellous (inner layer). Then, the model was imported into ANSYS Workbench 12.0 (ANSYS, Inc., Canonsburg, PA, USA). By using Workbench, the combined cortical-cancellous geometry was processed and two separate solids were produced. Then, the compound solid was exported to SolidWorks 2008 (SolidWorks Corp., Dassault Systemes, Concord, MA, USA) for further works. Figure 5.1 depicts the final CAD model of the femur in SolidWorks.

Fig. 5.1: The CAD model of intact bone [40]

As this study focuses on bone remodeling and bone density distribution in distal femur before and after total knee arthroplasty, the created model of the femur was cut below the diaphysis midsection using SolidWorks. Also, the condyles were resected so that the femoral component can be installed. Figure 5.2 depicts the resected femur including cortical (outer layer) and

cancellous (inner layer which is darker) components ready to use for installing the femoral component.

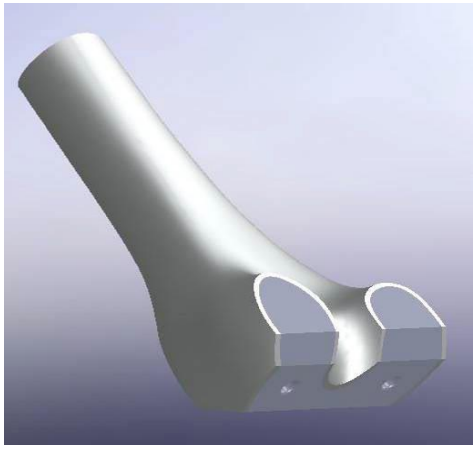

Fig. 5.2: The resected distal femur [40]

5.2 CAD model of the implant femoral component

The implant femoral component was developed via SolidWorks based on the commercial Duracon knee implant system (Stryker Corp., Kalamazoo, MI, USA). Figure 5.3 depicts the model of femoral component based on Duracon design.

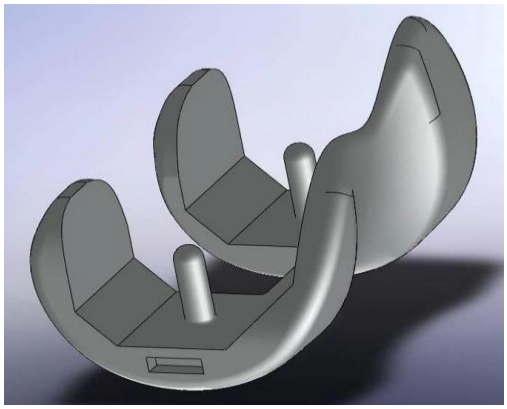

Fig. 5.3: The CAD model of femoral component [40]

CHAPTER 6 FINITE ELEMENT MODELLING

6.1 Introduction

Two three-dimensional finite element (FE) models are developed in this chapter using the software (ANSYS 12; ANSYS, Toronto, CA) to validate the thermodynamic-based theory of bone remodeling with morphological data of actual distal femur and the Strain Energy Density theory of bone remodeling developed previously by Huiskes *et al* [24]. Both theories, the Thermodynamic-based and the Strain Energy Density (SED), are coupled with the 3D Finite Element models to predict bone density distributions in the distal femoral bone before and after Total Knee Arthroplasty (TKA). The first model represents the intact distal femoral bone (Fig. 6.1a), the second one represents TKA using the femoral component of the Duracon knee implant system (Stryker Corp., Kalamazoo, MI, USA) which is made of cobalt-chromium-molybdenum (CoCrMo) alloy and connected this to the FE model of the intact femur (Fig. 6.1b). Fully bonded conditions are assumed at all interfaces.

(a) (b)

Fig. 6.1: The FE models (a) intact femur, (b) distal femur with femoral component

6.2 Material properties

6.2.1 Bone

According to Reilly *et al.* [132], cortical bone has transverse isotropy properties at the continuum level, whereas cancellous bone can be assumed to have orthotropic properties [133]. In this study, both types of simulated bone (cortical and cancellous) have been considered as linear

elastic homogeneous materials [134,135]. The initial values of the density used for the simulated cortical and cancellous bone are 1.64 g/cm^3 and 0.32 g/cm^3 [21], respectively. As discussed in section 4.8 the initial density of the composite bone is assumed to be equal to the average value of cortical and cancellous bones, meaning $\rho_0 = (0.32 + 1.64)/2 \approx 1$ (g/cm^3). It should be noted that a number of studies has shown that the initial bone density does not have an important influence on the final density distribution. Initially, the material properties of the composite bone depend on the initial value of bone density; after the first step, the properties are changed with changing the bone density [131]. The bone initially is considered as a linear isotropic material, and values of the elastic properties of the composite bone for the numerical simulation, used in this study as discussed in section4.8, are shown in table 6.1.

Table 6.1: Elastic properties of the composite bone given by [21]

E_{Old} (MPa)	E_{New} (MPa)	G_{Old} (MPa)	G_{New} (MPa)	υ
21000	14000	7778	5185	0.35

6.2.2 CoCrMo alloy

The femoral component of the Duracon knee system is made of cobalt-chromium-molybdenum (CoCrMo) alloy [136]. Properties of the CoCrMo alloy used in the Duracon system follow the ASTM (the American Society for Testing and Materials) standards for medical grade. These properties are shown in table 6.2.

Table 6.2: CoCrMo alloy properties [137-139]

Density (g/cc)	8.28	Elasticity	Linear elastic
Elastic modulus (GPa)	210	Isotropy	Isotropic
Yield strength (MPa)	827	Resistant to corrosion	High
Poisson's ratio	0.31	Biocompatibility	Very good

6.3 Element types

6.3.1 SOLID187 3-D 10-Node Tetrahedral Structural Solid

SOLID187 is a higher order 3D element and is used to simulate the femoral bone and the internal core. It has 10 nodes having three degrees of freedom at each node along with a quadratic displacement behaviour: translation in the nodal x, y, and z directions. Likewise, SOLID187 is well suited to modeling irregular meshes like those created by various CAD systems. It also has mixed formulation capability for simulating deformations of nearly incompressible elastoplastic materials, and fully incompressible hyperelastic materials. The SOLID187 element input data includes the orthotropic or anisotropic material properties. Orthotropic and anisotropic material directions correspond to the element coordinate directions. The geometry, node locations, and the coordinate system for this element are shown in Figure 6.2. Pressures may be input as surface loads on the element faces as shown by the circled numbers in Figure 6.2 [140].

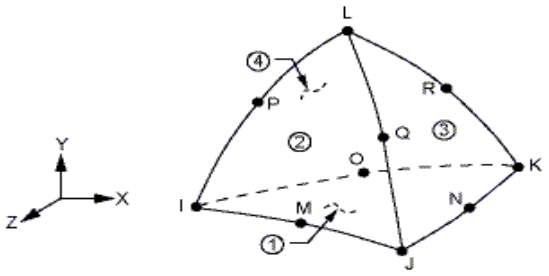

Fig. 6.2: SOLID187 element [140].

The element stress directions are parallel to the element coordinate system. The surface stress outputs are in the surface coordinate system and are available for any face as depicted in Figure 6.3 for face JIK coordinate system [140].

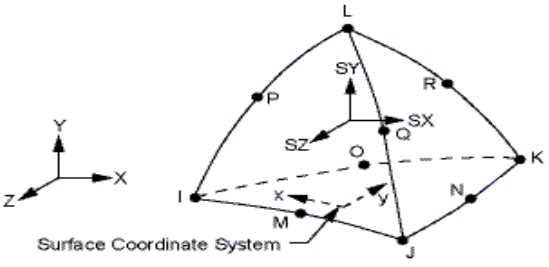

Fig. 6.3: SOLID187 Stress Output [140].

6.3.2 CONTA174 3D 8-node Surface-to-Surface Contact

CONTA174 is used to represent contact between 3D target surfaces (which will be described in the next section) and a deformable surface. It has three degrees of freedom at each node – translations in the nodal x, y, and z direction. This element is defined by eight nodes. It has the same geometric characteristics as the solid or shell element face with which it is connected. Contact occurs when the element surface penetrates one of the target segment elements (for example in this study TARGE170) on a specified target surface [141]. The geometry and node locations are depicted in Figure 6.4.

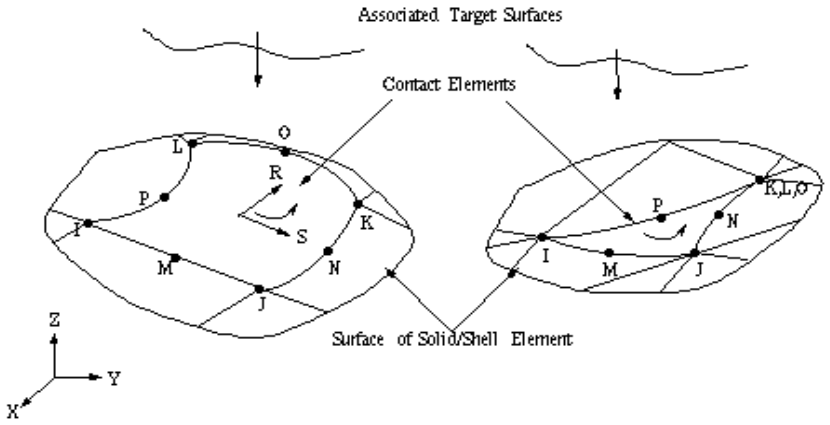

Fig. 6.4: CONTA174 element [141]

CONTA174 element is associated with the 3D target segment elements (for example TARGE170) through a shared real constant set. For rigid-flexible contact, the deformable surface must be represented by a contact surface [141].

6.3.3 TARGE170 3-D Target Segment

TARGE170 is used to represent various 3D target surfaces for the associated contact elements such as CONTA174. The contact elements themselves overlay the solid, shell, or line elements describing the boundary of a deformable body and are potentially in contact with the target surface, defined by TARGE170. This target surface is discretized by a set of target segment elements like TARGE170 and is paired with its associated contact surface via a shared real contact set [142].

For rigid target surfaces, TARGE170 elements can easily model complex target shapes. For flexible targets, these elements will overlay the solid, shell, or line elements describing the

boundary of the deformable target body. Therefore, the target surface can either be rigid or deformable. For modeling rigid-flexible contact, the rigid surface must be represented by a target surface. For flexible-flexible contact, one of the deformable surfaces must be overlayed by a target surface [142].

Each target surface can be associated with only one contact surface, and vice-versa. However, several contact elements could make up the contact surface and thus come in contact with the same target surface. Likewise, several target elements could make up the target surface and thus come in contact with the same contact surface. For either the target or contact surfaces, you can put many elements in a single target or contact surface, but doing so may increase computational cost. For a more efficient model, localize the contact and target surfaces by splitting the large surfaces into smaller target and contact surfaces, each of which contain fewer elements. If a contact surface may contact more than one target surface, you must define duplicate contact surfaces that share the same geometry but relate to separate targets, that is, that have separate real constant set numbers [142]. Figure 6.5 depicts the TARGE170 element.

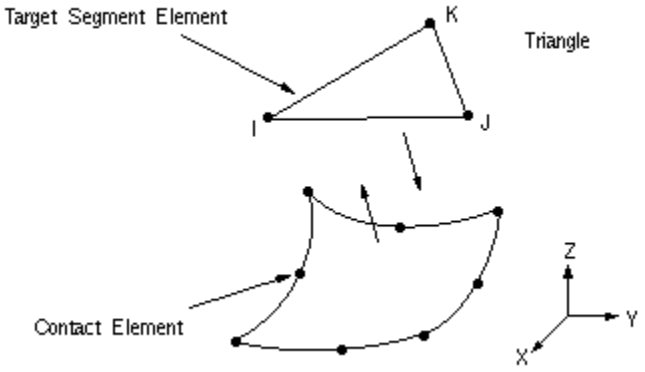

Fig 6.5: TARGE170 Target Surface Element [143].

6.4 Boundary and load conditions

The diaphysis midsection, including cortical and cancellous bone, is fixed for all DOF. As this study focuses on the prediction of evolution of bone density in the distal femoral bone using thermodynamic-based model, the axial (i.e. zero degree flexion) force was applied to each FE model. For that purpose, 3000N load which represents 3 to 4 times a body weight of 75 kg (as discussed in subsection 1.3.7) was applied equally on both condyles. The aforementioned loads

were distributed over several nodes that are located on the outer surfaces of both condyles and, at the same time, are in contact with UHMWPE articulating surface (the polymer part of the tibial component of the Duracon system which is not shown in Figure 6.6) in the direction of the femur's axial (i.e. zero degree flexion) to avoid stress concentration as shown in Figure 6.6.

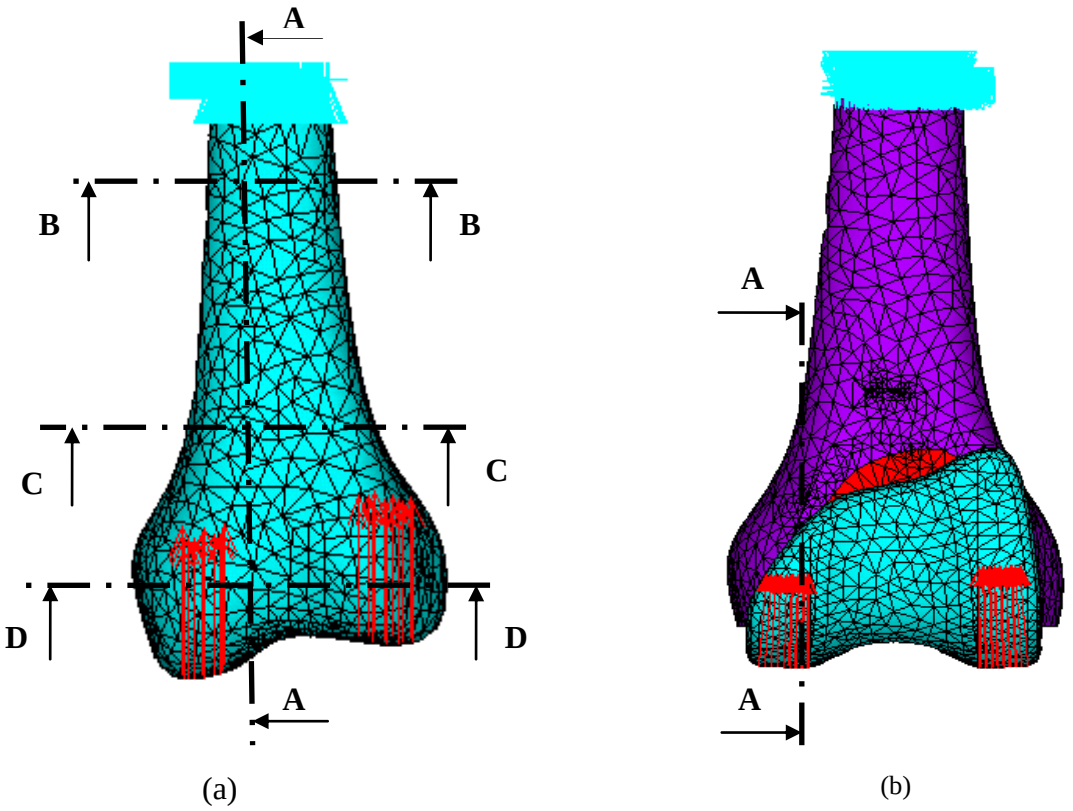

(a) (b)

Fig. 6.6: Boundary and load conditions on the (a) intact femur (b) femoral component of TKA

6.5 Further details of the FE models

The FE analysis of two models, i.e. the intact distal femoral bone and the implanted distal femoral bone using femoral component of Duracon knee implant system, were carried out. Two numerical codes were generated in ANSYS software and coupled with the two adaptive bone remodeling theories, i.e. the thermodynamic-based and the Strain Energy Density, to simulate bone remodeling in an intact distal femoral bone. This processes start from an initial bone density of 1 g/cm^3 and end with variable density distribution at the equilibrium condition. However, simulation of bone remodeling in an implanted bone was more complicated. First, the code used for thermodynamic-based theory was run using implanted distal femoral bone model with material properties of cortical bone rather than femoral implant properties, i.e. CoCrMo

alloy, to simulate the condition of bone before surgery. After 100 iterations, which is enough time to reach the density distribution equilibrium, the program was run for another 100 iterations using the material properties of CoCrMo alloy for femoral implant to simulate the adaptive bone remodeling after surgery. In other words, for the second model (i.e. the implanted distal femoral bone), the bone density of the intact bone at equilibrium (the results of the first 100 iterations) was used as starting point for TKA simulation. Since the results of the first run must be used for the second run without starting from the beginning of the program, another code was generated and coupled with the first one. Therefore, the simulation of density distribution in an implanted distal femoral bone using Thermodynamic-based theory of bone remodeling was created after 200 iterations.

CHAPTER 7 RESULTS AND DISCUSSION

7.1 Convergence of process

Since simulation of bone remodeling to predict bone density distribution using the thermodynamic-based model is an iterative process, Eq. 3.6 is considered as the convergence criterion for this process. As described in section 3.3, if the change in bone density is almost zero in any elements, the bone remodeling process ends and equilibrium is reached. As can be seen from Figure 7.1, in this study, the convergence of the variation of the density in all elements for both intact and implanted bone obtained after 50 iterations.

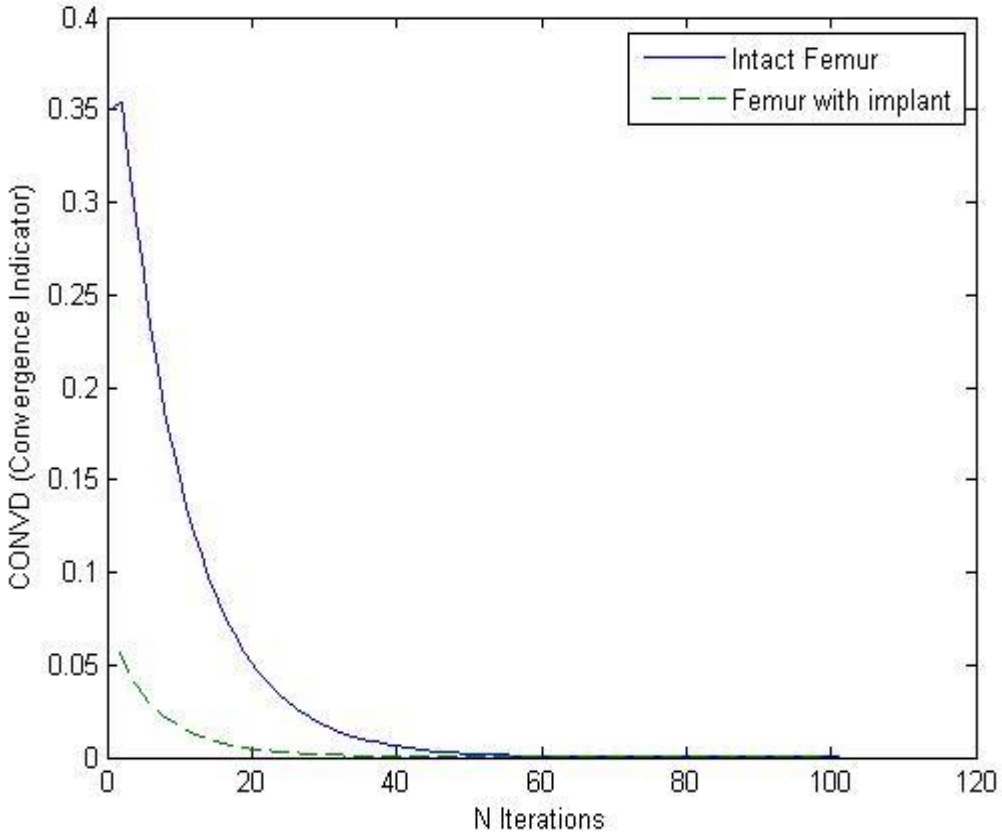

Fig. 7.1: Variation of change in bone density (CONVD) in all elements

7.2 Preoperative bone density distribution

To verify the thermodynamic-based theory, three numerical simulations were done. The first and the second simulations predict the evolution of bone density before and after TKA using the

thermodynamic-based model, while the third simulation used the strain energy density model developed previously by Huiskes *et al.* [24] to simulate bone density distribution before TKA.

The iterative process of bone remodeling started from an initial constant bone density and ended with variable density distribution at the equilibrium condition. The equilibrium condition was reached when no significant changes in density and elastic modulus of elements were observed. Figure 7.2c represents the simulation of density distribution in the intact distal femoral bone from the posterior view using thermodynamic-based model. Figure 7.2b shows the density distribution in the intact distal femoral bone from the posterior view based on the classical strain energy density model.

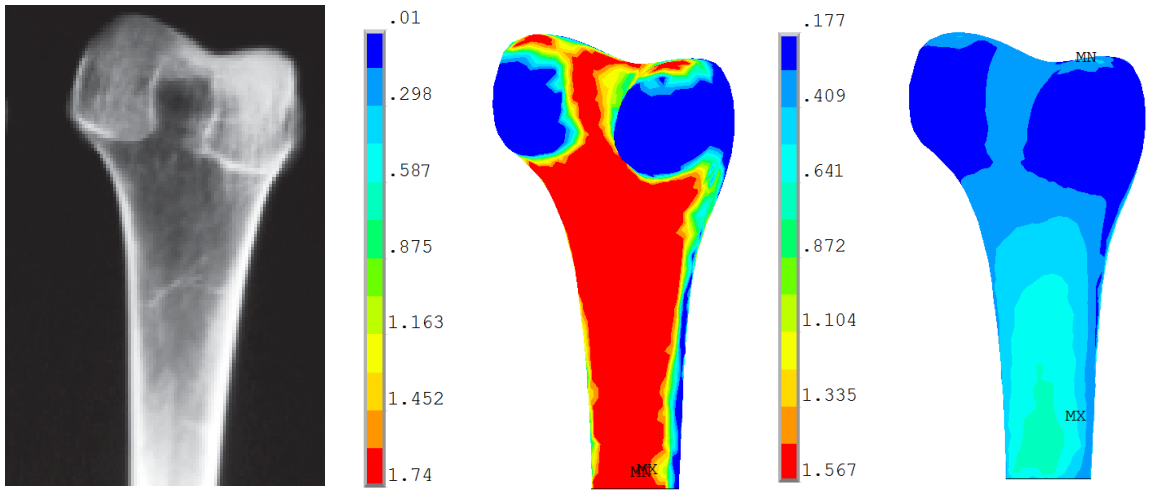

(a) **(b)** **(c)**

Fig. 7.2: The posterior view of the intact distal femur showing bone density distribution: (a) in clinical observation (X-ray) [144]. (b) simulated based on SED model. (c) simulated based on Thermodynamic-based model.

The architecture of the distal femoral bone was comparable. As clearly seen from Figure 7.2b and 7.2c, the patterns of bone density distribution are very similar. The dark blue zone shows less stress and consequently less density. The dark red zone demonstrates more stress and therefore more density. The mechanical loading affected areas on the both models have lighter blue color (denser), for the thermodynamic model, and red color, for the SED model, that means the densities in these areas are high (Fig. 7.2b and 7.2c). This indicates the region of the cortical bone. Also, the midsection area of thigh bone is the densest area according to both models because this region absorbs more stress due to the bending of the femur. However, two main

differences were observed. The first one is the range of values of bone density and the second difference is the shape of density distribution. It can be seen that the strain energy model overestimates the density distribution. This problem is revealed because in the classical model, the range of values of density varies between 0.01 and 1.74g/cm^3, whereas in the thermodynamic model these values depend on the parameters. The thermodynamic model predicts these limits, which depend on the parameters of the model, from the chemical kinetics reactions involved in bone resorption and apposition. It also can be due to the fact that the classical model considers only the mechanical loading as the stimulus in bone remodeling process, whereas the thermodynamic model takes into account the chemical reactions as well.

As it can be seen clearly, in the strain energy density model, the density has either minimum or maximum amount in all areas of the bone and does not show any gradualness in amount of density (Fig. 7.2b), whereas, in the thermodynamic-based model the density distributes gradually from a minimum amount in the distal femur to a maximum amount in the midsection of thigh bone (Fig. 7.2c), as it is in reality (Fig. 7.2a), therefore, it makes the proposed model more reliable to predict evolution of bone density near to the reality compare to SED model.

To verify the efficiency of proposed model, bone density distribution using the thermodynamic-based model was compared to the clinical observation, i.e. the X-ray image of posterior lower part of resected thigh bone (Fig. 7.2a). In general, the density changes were qualitatively similar to the clinical results in terms of regional bone loss or densification (Fig. 7.2a and 7.2c). As it can be seen in the X-ray image, the distal femur toward the midsection of the thigh bone becomes denser which is clearly consistent with the proposed model result (Fig. 7.2c) discussed in the previous paragraph.

Furthermore, same discussion can be made for the anterior view of the distal femur. Figure 7.3 represents the bone density distribution on the anterior surface of intact distal femur obtained from clinical observation (Fig. 7.3a) and two simulations using SED (Fig. 7.3b) and thermodynamic-based theory of bone remodeling (Fig. 7.3c).

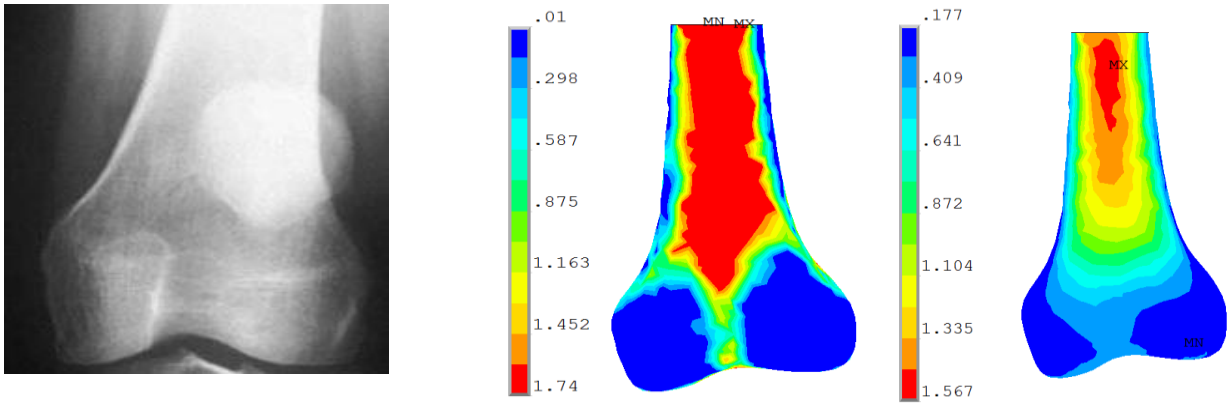

(a) (b) (c)

Fig. 7.3: The anterior view of the intact distal femur showing bone density distribution: (a) in clinical observation (X-ray) [145]. (b) simulated based on SED model. (c) simulated based on Thermodynamic-based model.

As it can be seen both models can predict the zones of high and low densities (i.e., cortical and cancellous bone) (Fig. 7.3b and 7.3c). However, the evolution of density in the thermodynamic-based model is gradual and more uniform than the SED, which makes the proposed model more realistic compared to the SED one. This claim can be verified by comparing simulated bone density distribution with X-ray image of a healthy distal femur (Fig. 7.3a). The latter demonstrates that the distal femur toward the midsection of the thigh bone becomes denser, as the thermodynamic-based model simulation displays (Fig. 7.3c)

For further details about the bone density distribution, four sections, namely, A-A, B-B, C-C, and D-D (Fig. 6.6a) were performed in the finite element model and then the sections were compared with each other as Figures 7.4-7.7 show. By comparing the density distribution in the sections of both models, it appears that the patterns are quite different, again, unlike the strain energy density model, the bone density distributions are more uniform and gradual in the thermodynamic-based model. Therefore, the thermodynamic-based model has more potential to predict the evolution of the bone density close to the reality.

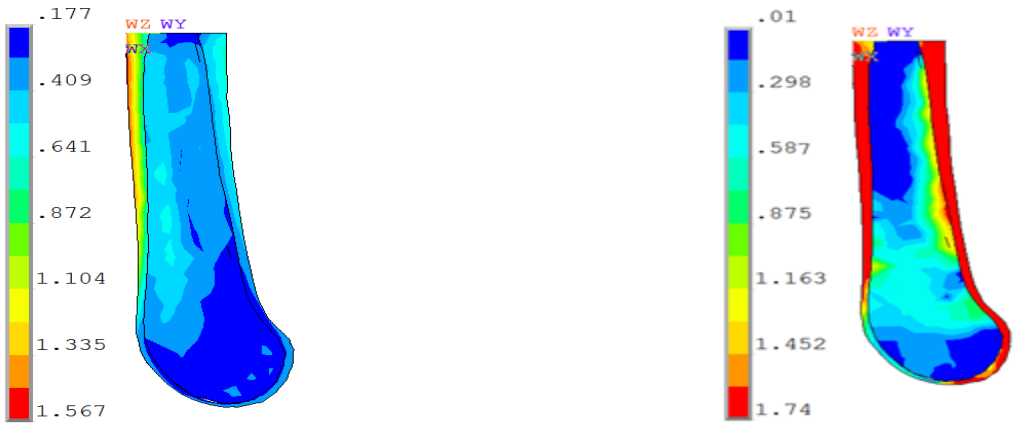

(a) (b)

Fig. 7.4: A-A section view of bone density distribution in the intact distal femur (Fig. 6.6a) simulated based on: (a) thermodynamic-based model, (b) SED model.

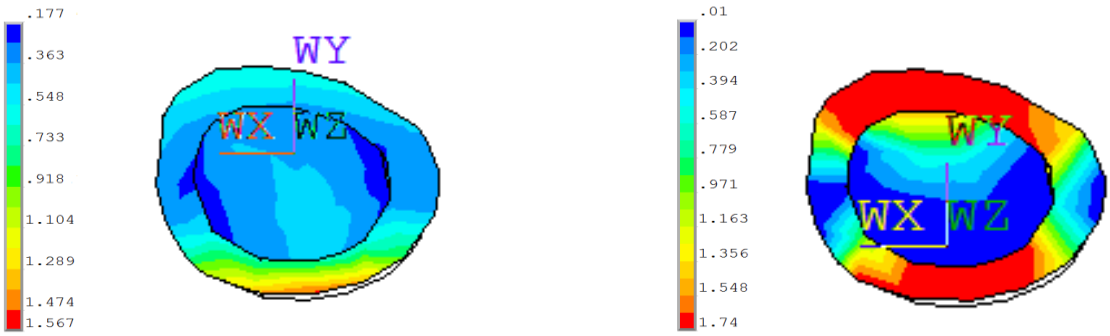

(a) (b)

Fig. 7.5: B-B section view of bone density distribution in the intact distal femur (Fig. 6.6a) simulated based on: (a) thermodynamic-based model, (b) SED model.

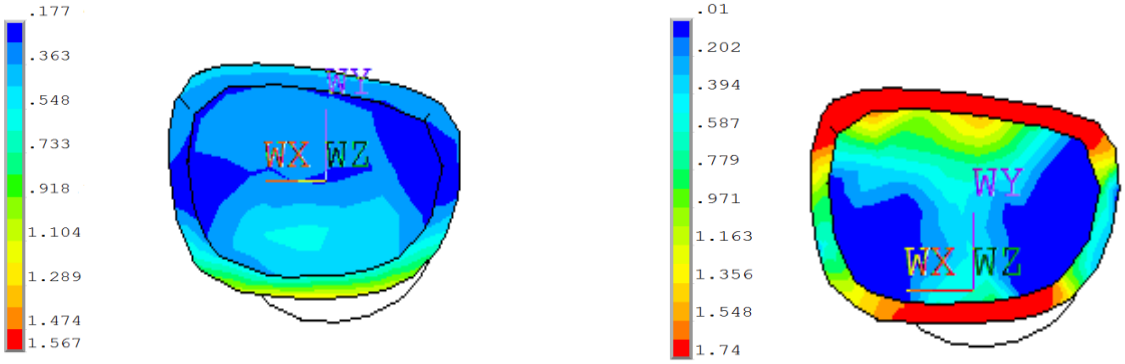

(a) (b)

Fig. 7.6: C-C section view of bone density distribution in the intact distal femur (Fig. 6.6a) simulated based on: (a) thermodynamic-based model, (b) SED model.

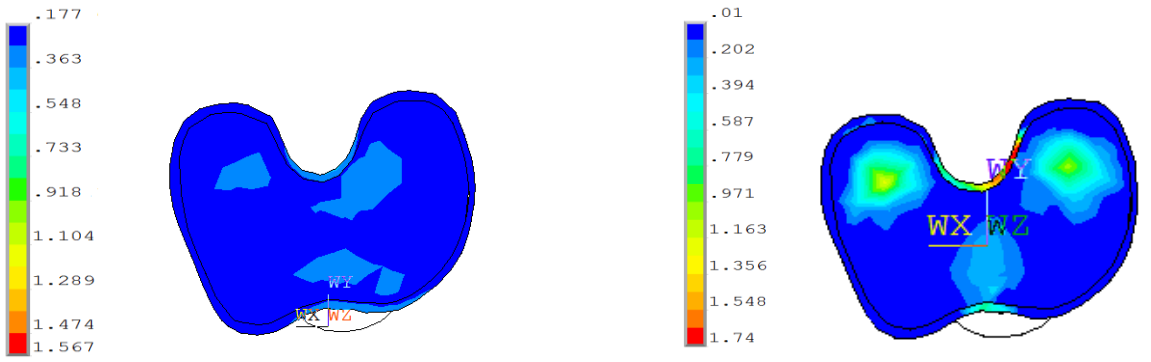

(a) (b)

Fig. 7.7: D-D section view of bone density distribution in the intact distal femur (Fig. 6.6a) simulated based on: (a) thermodynamic-based model, (b) SED model.

7.3 Postoperative bone density distribution after TKA

A numerical code was generated in ANSYS software to predict bone density distribution in the distal femoral bone using irreversible thermodynamic-based bone remodeling theory described by Eqs 4.26-4.38 after TKA as described in section 6.5. The equilibrium condition was reached when no significant changes in density and elastic modulus of elements were observed. Figure 7.8 represents simulation of the density distribution in the distal femoral bone from the posterior view (Fig. 7.8a) and A-A section view (Fig. 7.8b) based on the irreversible thermodynamic-based theory of bone remodeling after TKA.

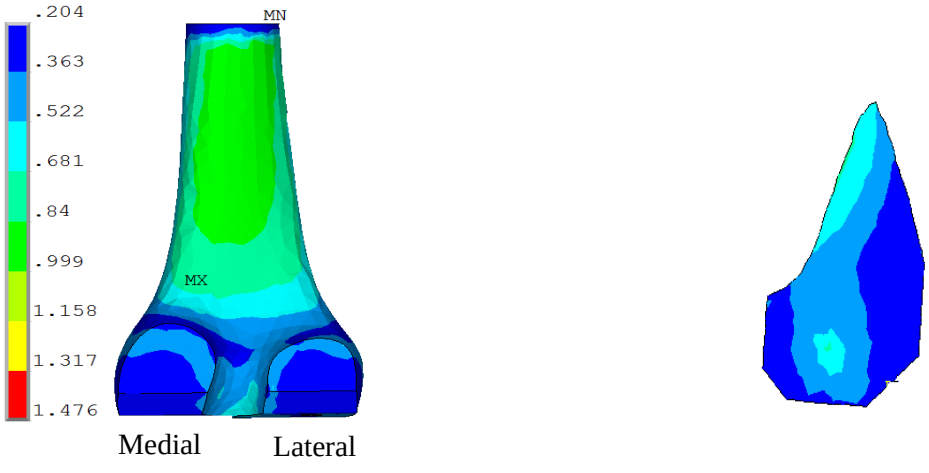

(a) **(b)**

Fig. 7.8: Simulation of density distribution in a distal femoral bone after TKA using the thermodynamic-based theory: (a) from the posterior view, (b) A-A section view (depicted in Fig. 6.6b).

These results were compared with the results obtained by Van Lenthe *et al.* [17], who investigated bone resorption in distal femoral bone after TKA using the SED model of bone remodeling (Fig. 7.9). Van Lenthe *et al.* divided the distal femoral bone in five regions of interest (ROI) as Figure 7.9a shows. They found that the most bone loss was predicted in the anterior distal ROI (No. 1) (Fig. 7.9b), which is consistent with the result of the proposed theory (blue region in the anterior distal region in Fig. 7.8b). Also, by comparing Fig. 7.8a and Fig. 7.9c, one can notice that bone loss is greater in the lateral than the medial condyle for both models. In other words, the bone density is lesser in the lateral than the medial condyle for both models. These results show that the proposed model (the thermodynamic-based model) is quite comparable with the strain energy density model.

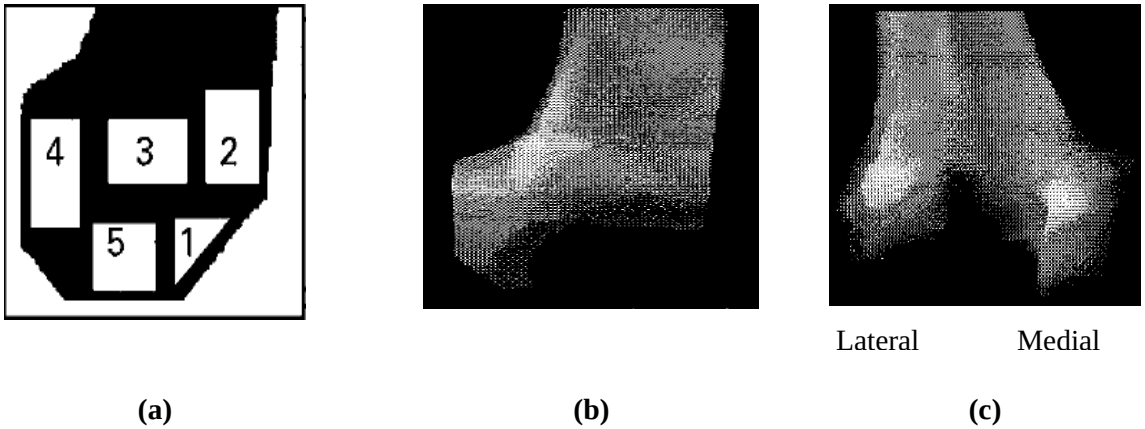

Fig. 7.9: (a) Distal femur regions marked into 'zones' by Van Lenthe *et al.* [17], (b) Simulated lateral DEXA scans obtained by Van Lenthe *et al.* [17], (c) Simulated frontal DEXA scans obtained by Van Lenthe *et al.* [17].

Furthermore, to verify the postoperative results of the proposed theory of bone remodeling, the current bone configuration was compared to the results of clinical observations obtained by Mintzer *et al.* [6] (Fig. 7.10). They marked out zones in the distal femur as shown in Figure 7.10a. According to Mintzer *et al.*'s investigation [6], bone loss was most frequently detected in zones 1, 2, and 3 of the anterior femur, as postoperative follow up radiograph shows in Figure 7.10b. By comparing this result with the simulation of evolution of bone density after TKA using the thermodynamic-based theory (Fig. 7.10c), it is proved that the proposed theory is well consistent with the reality, because the most bone loss in both clinical observation and the FE model has occurred in the anterior region of distal femur.

(a) **(b)** **(c)**

Fig. 7.10: (a) Distal femur regions marked into 'zones' by Mintzer et al. [6], (b) Postoperative follow up radiograph showing Lateral view of a distal femoral bone from Mintzer et al. [6], (c) Predicted bone density distribution after TKA simulated based on thermodynamic-based model.

7.4 Further verification

From the results obtained, the FE study using the thermodynamic-based theory of bone remodeling confirms that the anterior region indeed has the least density among all regions in the distal femur after TKA (Fig. 7.10c). This fact has been supported by Mahboob [40] in his thesis but in term of stress. Mahboob has showed that the anterior region experiences the least loading and most shielded from loading stresses under among all regions in the distal femur as Figure 7.11a depicts, so did Cameron and Cameron [95], Mintzer *et al.* [6], and van Loon *et al.* [146] (Fig. 7.11b).

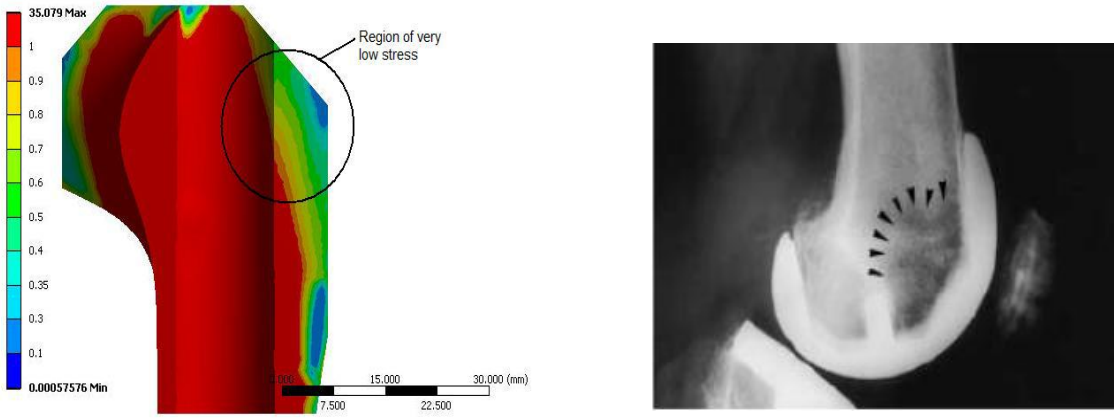

(a) **(b)**

Fig. 7.11: (a) Stress-shielded region in the anterior distal femur obtained by Mahboob [40], (b) X-ray radiograph from van Loon et al. showing Stress-shielded region in the anterior distal femur [146].

CHAPTER 8 CONCLUSIONS AND LIMITATIONS

Bone remodeling is a complex process in which mechanical, chemical, and biological parameters have the main role for initiating, continuing, and ending the process. It is, also, an important factor that leads to bone resorption in the surrounding distal femoral bone. Therefore, taking this factor into account in the design of knee implants is clinically very important, because based on it the bone density distribution can be predicted after total knee arthroplasty (TKA).

In this investigation, a new bone remodeling theory based on thermodynamics principles proposed by Bougherara *et al.* [21] was implemented to predict the bone density distribution in distal femoral bone before and after TKA. This theory considers mechanical, chemical, and biological factors as stimuli for bone formation and resorption. This model was applied to calculate the time evolution of bone density in different parts of a healthy distal femoral bone, as well as distal femoral bone with a prosthetic implant. Numerical simulations of bone density distributions agreed very well with clinical data (X-rays) of a healthy distal femur and implanted femur. On the other hand, the numerical simulations of bone density distribution in the distal femur resulted from the thermodynamic-based model show that the bone density distributes gradually from a minimum amount in the distal femur to a maximum amount in the midsection of thigh bone. This finding is consistent with the clinical observations.

During the investigation, several limitations came across. Numerical studies are based on static analyses of the bone-implant system and dynamic analyses of the models were not included in the study to determine the bone density distribution. Also, this investigation was limited only to comparing density distribution under a load representative of 3 to 4 times the body weight (3000N) considering as an axial force transmitted through the knee joint during regular gait. It should be considered that a static analysis applying an axial average body weight force with relevant constraints is quite sufficient to investigate verification of a new adaptive bone remodeling theory, i.e. Thermodynamic-based theory, in the distal femoral bone which is the aim of this study. Also, this study has been performed on a rather idealized static scenario incorporating only one knee flexion angle. Surely, a dynamic study that includes all ligaments and muscles forces input on the joint considering different angle of flexion and extension during normal gait would be useful – and this may well be an area of further research, but it is

nonessential for the purposes of this study. Likewise, Duracon system was used as the femoral component of knee implant and the effect of changing the design of femoral component was not examined which could be another area of further research.

Only the distal part of the femur was modelled. It is better to consider the whole geometry of the femur and the tibia as well. Finally, although this investigation was based on theoretical study, no doubt an experimental, for example an *in vivo* biomechanics, study of bone adaptation will further establish the potential for thermodynamic-based theory of bone remodeling which can be again another base for future researches.

Appendix

The five kinetic chemical equations that describe the remodeling are as follow [21]:

$\dot{\mathrm{N}}_{\mathrm{MCELL}} = \frac{\partial \mathrm{N}_{\mathrm{MCELL}}}{\partial \tau} = -\delta_1(\beta_1 + \mathrm{N}_{\mathrm{MCELL}})\mathrm{N}_{\mathrm{MCELL}} + \mathrm{J}_3 + \mathrm{J}_{\mathrm{New\_B}} - \mathrm{D}_1$
$\dot{\mathrm{N}}_{\mathrm{Old\_B}} = \frac{\partial \mathrm{N}_{\mathrm{Old\_B}}}{\partial \tau} = -\big(\beta_3 - \mathrm{N}_{\mathrm{MCELL}} + \mathrm{N}_{\mathrm{Old\_B}} + \mathrm{N}_{\mathrm{Activ\_B}} + \mathrm{N}_{\mathrm{Osteoid}} + \mathrm{N}_{\mathrm{New\_B}}\big)\mathrm{N}_{\mathrm{Old\_B}} - \delta_3\big[\beta_7 - \mathrm{N}_{\mathrm{Old\_B}} - 2\big(\mathrm{N}_{\mathrm{Activ\_OB}} + \mathrm{N}_{\mathrm{Osteoid}} + \mathrm{N}_{14}\big)\big]\mathrm{N}_{\mathrm{Old\_B}} + 2\mathrm{J}_{\mathrm{New\_B}} - \mathrm{D}_2 - \mathrm{D}_3$
$\dot{N}_{Activ\_B} = \frac{\partial N_{Activ\_B}}{\partial \tau} = \delta_3(\beta_7 - N_{Old\_B} - 2\big(N_{Active\_B} + N_{Osteoid} + N_{New\_B}\big)N_{Old\_B} - \delta_4\big(\beta_{10} - N_{Osteoid} - N_{New\_B}\big)N_{Active\_OB} + D_3 - D_4$
$\dot{\mathrm{N}}_{\mathrm{Osteoid}} = \frac{\partial \mathrm{N}_{\mathrm{Osteoid}}}{\partial \tau} = \delta_4\big(\beta_{10} - \mathrm{N}_{\mathrm{Osteoid}} - \mathrm{N}_{\mathrm{New\_B}}\big)\mathrm{N}_{\mathrm{Activ\_OB}} - \delta_5(\beta_{13} - \mathrm{N}_{\mathrm{New\_B}})\mathrm{N}_{\mathrm{Osteoid}} + \mathrm{D}_4 - \mathrm{D}_5$
$\dot{\mathrm{N}}_{\mathrm{New\_B}} = \frac{\partial \mathrm{N}_{\mathrm{New\_B}}}{\partial \tau} = \delta_5(\beta_{13} - \mathrm{N}_{\mathrm{New\_B}})\mathrm{N}_{\mathrm{Osteoid}} - \mathrm{J}_{\mathrm{New\_B}} + \mathrm{D}_5$

These differential equations are the dimensionless form of Eq. 4.26. The scaling variables are as follow [21]:

$\tau = tk_{+2}n_{B0},$	$N_i = \frac{n_i}{n_{B0}},$	$\delta_\rho = \frac{k_{+\rho}}{k_{+2}},$
$\beta_i = \frac{B_i}{n_{B0}},$	$D_\rho = \frac{l_{\rho v} d_{(1)}}{k_{+2} n^2_{B0}},$	$J_i = \frac{j_i}{k_{+2} n^2_{B0}},$

where τ is time, $\mathrm{N_i}$ is the rate of concentration of ith substance, δ_ρ is the ratio of rate of ρth reaction to second reaction, $\mathrm{D_\rho}$ is the parameter that describes the influence of dynamical loading on rate of ρth chemical reaction, β_i is the concentration of the ith substance

and n_{B0} is the sum of initial molar concentration of relevant substances and j_i are fluxes of substances.

The remaining substances are calculated using the following relations [12]:

$$B_1 = n_1 - n_2$$

$$B_3 = n_3 + n_2 - n_5 - n_8 - n_{11} - n_{14}$$

$$B_7 = n_7 + n_5 + 2n_8 + 2n_{11} + 2n_{14}$$

$$B_{10} = n_{10} + n_{11} + n_{14}$$

$$B_{13} = n_{13} + n_{14}$$

References

[1] Bartel, D.L., Davy, D.T., and Keaveny, T.M., 2006. *"Orthopaedic Biomechanics: Mechanics and Design in Musculoskeletal Systems,"* Pearson Prentice Hall, Upper Saddle River, NJ. 370 p. ISBN 0-13-008909-5.

[2] Chen, E., Ellis, R. E., Bryant, J. T., Rudan, J. F., 2001. "A computational model of postoperative knee kinematics ," *Medical Image Analysis,* **5** (4), pp. 317-330.

[3] Hill, P. A., 1998. "Bone remodeling," *British Journal of Orthopaedics,* **25**(2), pp. 101–107.

[4] Frankel, V. H., 1980. "*Basic biomechanics of the skeletal system*," Philadelphia: Lea & Febiger, 303 p. ISBN: 081210708X.

[5] Ruimerman, R., 2005. "Modeling and Remodeling in Bone Tissue," Ph.D. Thesis, Technische Universiteit, Eindhoven.

[6] Mintzer, C. M., Robertson, D. D., Rackemann, S., Ewald, F. C., Scott, R. D., and Spector, M., 1990. "Bone Loss in the Distal Anterior Femur After Total Knee Arthroplasty," *Clinical Orthopaedics and Related Research,* (260) pp. 135-143.

[7] Completo, A., Fonseca, F., and Simões, J. A., 2008. "Strain Shielding in Proximal Tibia of Stemmed Knee Prosthesis: Experimental Study," *Journal of Biomechanics,* **41**(3) pp. 560-566. DOI: 10.1016/j.jbiomech.2007.10.006.

[8] Gefen, A., 2002. "Computational simulations of stress shielding and bone resorption around existing and computer-designed orthopaedic screws." *Medical and Biological Engineering and Computing*, **40**(3), pp. 311-322.

[9] Petersen, M. M., Olsen, C., Lauritzen, J. B., and Lund, B., 1995. "Changes in Bone Mineral Density of the Distal Femur Following Uncemented Total Knee Arthroplasty," *The Journal of Arthroplasty,* **10**(1) pp. 7-12.

[10] Tayton, K., Phillips, G., and Ralis, Z., 1982. "Long-Term Effects of Carbon Fibre on Soft Tissues," *Journal of Bone and Joint Surgery (British),* **64**(1) pp. 112-114.

[11] Huiskes, R., Weinans, H., Grootenboer, H. J., Dalstra, M., Fudala, B., and Slooff, T. J., 1987. "Adaptive Bone-Remodeling Theory Applied to Prosthetic-Design Analysis," *Journal of Biomechanics,* **20**(11-12) pp. 1135-1150.

[12] Huiskes, R., Weinans, H., and Van Rietbergen, B., 1992. "The Relationship between Stress Shielding and Bone Resorption Around Total Hip Stems and the Effects of Flexible Materials," *Clinical Orthopaedics and Related Research,* (274) pp. 124-134.

[13] American Association of Hip and Knee Surgeons, 2007. "Knee Implants," *www.aaos.org.* American Academy of Orthopaedic Surgeons, Accessed June 1, 2010, <http://orthoinfo.aaos.org/topic.cfm?topic=A00221>.

[14] Gupta, S. K., Chu, A., Ranawat, A. S., Slamin, J., and Ranawat, C. S., 2007. "Review Article: Osteolysis After Total Knee Arthroplasty," *The Journal of Arthroplasty,* **22**(6) pp. 787-799. DOI: 10.1016/j.arth.2007.05.041.

[15] Naudie, D. D. R., Ammeen, D. J., Engh, G. A., and Rorabeck, C. H., 2007. "Wear and Osteolysis Around Total Knee Arthroplasty," *Journal of the American Academy of Orthopaedic Surgeons,* **15**(1) pp. 53-64.

[16] Cadambi, A., Engh, G. A., Dwyer, K. A., and Vinh, T. N., 1994. "Osteolysis of the Distal Femur After Total Knee Arthroplasty," *The Journal of Arthroplasty,* **9**(6) pp. 579-594. DOI: DOI: 10.1016/0883-5403(94)90111-2.

[17] Van Lenthe, G. H., De Waal Malefijt, M. C., and Huiskes, R., 1997. "Stress Shielding After Total Knee Replacement may Cause Bone Resorption in the Distal Femur," *Journal of Bone and Joint Surgery (British),* **79**(1) pp. 117-122.

[18] Angelides, M., Chan, K., Ahmed, A. M., and Joly, L., 1988. "Effect of Total Knee Arthroplasty on Distal Femur Stresses," *Transactions of the Orthopaedic Research Society,* **13** pp. 475.

[19] Lonner, J. H., Klotz, M., Levitz, C., and Lotke, P. A., 2001. "Changes in Bone Density After Cemented Total Knee Arthroplasty: Influence of Stem Design," *The Journal of Arthroplasty,* **16**(1) pp. 107-111. DOI: 10.1054/arth.2001.16486.

[20] Sathappan, S., Pang, H., Manoj, A., Ashwin, T., and Satku, K., 2009. "Does Stress Shielding Occur with the use of Long-Stem Prosthesis in Total Knee Arthroplasty?" *Knee Surgery, Sports Traumatology, Arthroscopy,* **17**(2) pp. 179-183. DOI: 10.1007/s00167-008-0649-0.

[21] Bougherara H, Klika V, Marsik F, Marik IA, Yahia L., 2010.“ New predictive model for monitoring bone remodeling,” *Journal of Biomedical Materials Research part A,* **95**A (1) pp. 9-24. DOI: 10.1002/jbm.a.32679.

[22] Weinans, H., Huiskes, R., Grootenboer, H. J., 1992. “The behavior of adaptive bone-remodeling simulation models,” *Journal of Biomechanics,* **25** (12) pp. 1425-1441.

[23] Frost, H. M., 1998. “Changing Concepts in Skeletal Physiology: Wolff's Law, the Mechanostat, and the "Utah Paradigm",” *American Journal of Human Biology,* **10** (5) pp. 599-605

[24] Huiskes, R., Rulmerman, R., Van Lenthe, G. H., Janssen, J. D., 2000. “Effects of mechanical forces on maintenance and adaptation of form in trabecular bone,” *Nature* **405** (6787), pp. 704-706

[25] Orr, T., 1990. “The role of mechanical stresses in bone remodeling,” Ph.D. Thesis, Stanford University.

[26] Canadian Institute for Health Information (CIHI), 2009. *"Canadian Joint Replacement Registry (CJRR) 2008 Annual Report: Hip and Knee Replacements in Canada,"* CIHI and Canadian Orthopaedic Association, Ottawa, ON. ISBN 978-1-55465-189-4, Available at http://secure.cihi.ca/cihiweb/dispPage.jsp?cw_page=AR_30_E.

[27] The center for orthopaedics and sports medicine, 2003. “KNEE JOINT-ANATOMY & FUNCTION,” *www.arthroscopy.com*. Accessed May 21, 2010, http://www.arthroscopy.com/sp05001.htm

[28] Martini, F.H., Timmons, M.J., and Tallitsch, R.B., 2008. *"Human Anatomy,"* 6th Edition. Pearson Benjamin Cummings, Upper Saddle River, NJ. 869 p. ISBN 978-0321-51197-3.

[29] Fitt, S.S., 1996. *"Dance Kinesiology,"* 2nd Edition. Schirmer Books, New York, NY. 484 p. ISBN 0-02-864507-3.

[30] Medical multimedia Group, LLC, 2009. “Adult knee: patient Guides,” *www.eorthopod.com*. Accessed May 21, 2010, http://www.eorthopod.com/adult-knee-patient-guides

[31] Tortora, G. J., 2004. “*Introduction to the human body: the essentials of anatomy and physiology*,” 6th edition, John Wiley and Sons, NJ, 689 p., ISBN: 9780470120170

[32] Reilly, D. T., and Burstein, A. H., 1974. "The Mechanical Properties of Cortical Bone," *Journal of Bone and Joint Surgery (American),* **56**(5) pp. 1001-1022.

[33] Kopperdahl, D. L., and Keaveny, T. M., 1998. "Yield Strain Behavior of Trabecular Bone," *Journal of Biomechanics,* **31**(7) pp. 601-608. DOI: 10.1016/S0021-9290(98)00057-8.

[34] Linde, F., and Hvid, I., 1989. "The Effect of Constraint on the Mechanical Behaviour of Trabecular Bone Specimens," *Journal of Biomechanics,* **22**(5) pp. 485-490. DOI: 10.1016/0021-9290(89)90209-1.

[35] Ashman, R. B., Rho, J. Y., and Turner, C. H., 1989. "Anatomical Variation of Orthotropic Elastic Moduli of the Proximal Human Tibia," *Journal of Biomechanics,* **22**(8-9) pp. 895-900. DOI: 10.1016/0021-9290(89)90073-0.

[36] Rohlmann, A., Zilch, H., Bergmann, G., and Kolbel, R., 1980. "Material Properties of Femoral Cancellous Bone in Axial Loading. PartI: Time-Independent Properties," *Archives of Orthopaedic and Trauma Surgery,* **97**(2) pp. 95-102.

[37] Lawson, W., Duric, Z., 2009. “Analyzing human gait using patterns of translation and rotation,” *Lecture Notes in Computer Science (including subseries Lecture Notes in Artificial Intelligence and Lecture Notes in Bioinformatics),* 5627 LNCS, pp. 408-417.

[38] Gage, J. R., 1990. "An Overview of Normal Walking," *Instructional Course Lectures,* **39** pp. 291-303.

[39] Deluzio, K., "Gait Analysis," *Mechanical and Materials Engineering, Faculty of Applied Science.* Queen's University, Kingston, ON. Accessed July 8, 2010, <http://me.queensu.ca/people/deluzio/GaitAnalysis.php>.

[40] Mahboob, Z., 2009. "A validated finite element study of stress shielding in a novel hybrid knee implant," M.A.Sc. Thesis, Ryerson University, Toronto.

[41] Thompson, D. M., 2002. "Introduction to the Study of Human Walking: Basics of Gait Terminology," *Lectures on the Control of Human Movement.* Department of Biostatics and Epidemiology, University of Oklahoma Health Sciences Centre, Accessed June 5, 2010, <http://moon.ouhsc.edu/dthompso/gait/terms.htm>.

[42] Kaufman, K.R., and Sutherland, D.H., 2006. "Kinematics of Normal Human Walking: Gait events," in *Human Walking,* J. Rose and J. G. Gamble (eds). 3rd Ed. Lippincott Williams & Wilkins, Philadelphia, PA. pp. 39-42, Chap. 3. ISBN 0-7817-5954-4.

[43] Clarke, H.D., Scott, W.N., Insall, J.N., Pedersen, H.B., Math, K.R., Vigorita, V.J., and Cushner, F.D., 2001. "Anatomy: Motion and Function," in *Surgery of the Knee,* J. N. Insall and W. N. Scott (eds). (Vol. 1) 3rd Ed. Churchill Livingstone, New York, NY. pp. 1301-1306, Chap. 9. ISBN 0-443-06545-4 (set).

[44] Andriacchi, T. P., and Alexander, E. J., 2000. "Studies of Human Locomotion: Past, Present and Future," *Journal of Biomechanics,* **33**(10) pp. 1217-1224. DOI: 10.1016/S0021-9290(00)00061-0.

[45] Winter, D. A., 1980. "Overall Principle of Lower Limb Support during Stance Phase of Gait," *Journal of Biomechanics,* **13**(11) pp. 923-927.

[46] Sutherland, D. H., Olshen, R., Cooper, L., and Woo, S. L., 1980. "The Development of Mature Gait," *Journal of Bone and Joint Surgery (American),* **62**(3) pp. 336-353.

[47] Morrison, J. B., 1970. "The Mechanics of the Knee Joint in Relation to Normal Walking," *Journal of Biomechanics,* **3**(1) pp. 51-61. DOI: 10.1016/0021-9290(70)90050-3.

[48] Denham, R. A., and Bishop, R. E., 1978. "Mechanics of the Knee and Problems in Reconstructive Surgery," *Journal of Bone and Joint Surgery (British),* **60-B** (3) pp. 345-352.

[49] Morrison J.B., 1969. "Function of the knee joint in various activities," *Bio-Medical Engineering,* **4**(12) pp. 573-580.

[50] Kuster, M. S., Wood, G. A., Stachowiak, G. W., Gächter, A., 1997. "Joint load considerations in total knee replacement," *Journal of Bone and Joint Surgery - Series B,* **79**(1), pp. 109-113.

[51] Harrington, I. J., 1967. "A bioengineering analysis of force actions at the knee in normal and pathological gait," *Bio-Medical Engineering,* **11(**5) pp. 167-172.

[52] Collins, J. J., 1995. "The redundant nature of locomotor optimization laws," *Journal of Biomechanics,* **28(**3) pp.251-267.

[53] Andriacchi, T. P., Andersson, G. B. J., Fermier, R. W., 1980. "A study of lower-limb mechanics during stair-climbing," *Journal of Bone and Joint Surgery - Series A,* **62** (5) pp. 749-757.

[54] Ellis, M. I., Seedhom, B. B., 1984. "Wright V. Forces in the knee joint whilst rising from a seated position," *Journal of Biomedical Engineering*, **6**(2) pp.113-120.

[55] Nisell, R., 1985. "Mechanics of the knee. A study of joint and muscle load with clinical applications," *Acta Orthopaedica Scandinavica, Supplement* 216 pp. 1-42.

[56] Dahlkvist, N. J., Mayo, P., Seedhom, B. B., 1982. "Forces during squatting and rising from a deep squat," *Engineering in Medicine*, **11**(2) pp. 69-76.

[57] Collins, J. J., 1994. "Antagonistic synergistic muscle action at the knee during competitive weightlifting," *Medical and Biological Engineering and Computing*, **32**(2) pp. 168-174.

[58] Clarke, H.D., Scott, W.N., Insall, J.N., Pedersen, H.B., Math, K.R., Vigorita, V.J., and Cushner, F.D., 2001. "Anatomy: Motion and Function," in *Surgery of the Knee,* J. N. Insall and W. N. Scott (eds). (Vol. 2) 3rd Ed. Churchill Livingstone, New York, NY. pp. 1821-1825, Chap. 79. ISBN 0-443-06545-4 (set).

[59] Ferguson, W., 2007. "Excision of the Knee Joint. Recovery with a False Joint and a Useful Limb," *Medical Times Gazette,* **1** pp. 601, 1861.

[60] Campbell, W. C., 2005. "The Classic: Interposition of Vitallium Plates in Arthroplasties of the Knee - Preliminary Report (1940)," *Clinical Orthopaedics and Related Research,* **440** pp. 22-23.

[61] Speed, J. S., Trout, P. C., 2007, "Arthroplasty of the knee: A follow-up study," *Journal of Bone and Joint Surgery*, **31**(B) pp. 53, 1949.

[62] Miller, A., Friedman, B., 1952. "Fascial arthroplasty of the knee," *The Journal of bone and joint surgery. American volume,* **34**A (1) pp. 55-63.

[63] Macintosh, D. L., 1958. "Hemiarthroplasty of the knee using a space occupying prosthesis for painful varus and valgus deformities," *The Journal of bone and joint surgery. American volume,* **40**A pp.1431.

[64] Emerson Jr., R. H., Potter, T., 1985. "The use of the McKeever metallic hemiarthroplasy for unicompartmental arthritis," *Journal of Bone and Joint Surgery - Series A,* **67** (2) pp. 208-212.

[65] McKeever, D. C., 2005. "The Classic: Tibial Plateau Prosthesis (1960)," *Clinical Orthopaedics and Related Research,* Springer, **440** pp. 4-8. DOI: 10.1097/01.blo.0000187336.17627.ea.

[66] Carr, B. C., and Goswami, T., 2009. "Knee Implants – Review of Models and Biomechanics," *Materials & Design,* **30**(2) pp. 398-413. DOI: 10.1016/j.matdes.2008.03.032.

[67] Gunston, F. H., 1971. "Polycentric knee arthroplasty. Prosthetic simulation of normal knee movement," *Journal of Bone and Joint Surgery - Series B,* **53**(2) pp. 272-277.

[68] Scott, R.D., 2006. *"Total Knee Arthroplasty,"* Saunders Elsevier, Philadelphia, PA. 148 p. ISBN 978- 0-7216-3948-2.

[69] Shiers, L. G. P., 1954. "Arthroplasty of the knee: Preliminary report of a new method," *The Journal of bone and joint surgery. British volume,* **36** pp. 553-560.

[70] Robinson, R. P., 2005. "The Early Innovators of Today's Resurfacing Condylar Knees," *The Journal of Arthroplasty,* **20**(Supplement 1) pp. 2-26. DOI: 10.1016/j.arth.2004.11.002.

[71] Swanson, S. A., and Freeman, M. A., 1972. "A New Prosthesis for the Total Replacement of the Knee." *Acta Orthopaedica Belgica,* **38, Suppl. 1** pp. 55-62.

[72] Swanson, S. A. V., and Freeman, M. A. R., 1974. "The Design of a Knee Joint Implant," *Bio-Medical Engineering,* **9**(8) pp. 348-352.

[73] Yamamoto, S., 1979. "Total Knee Replacement with the Kodema-Yamamoto Knee Prosthesis," *Clinical Orthopaedics and Related Research,* **145** pp. 60-67.

[74] Hungerford, D. S., Kenna, R. V., and Krackow, K. A., 1982. "The Porous-Coated Anatomic Total Knee," *Orthopedic Clinics of North America,* **13**(1) pp. 103-122.

[75] Carpenter Technology Corporation, "Technical Datasheet: BioDur® CCM Plus® Alloy," *Carpenter Tech Centre (Cartech.com).* CRS Holdings Inc, Reading, PA. Accessed June 22, 2010, <http://www.cartech.com/techcenter.aspx?id=1692>

[76] Tokash, J. C., Stojilovic, N., Ramsier, R. D., Kovacik, M. W., and Mostardi, R. A., 2005. "Surface Analysis of Prosthetic Wear Debris," *Surface and Interface Analysis,* **37**(4) pp. 379-384. DOI: 10.1002/sia.1993.

[77] Paul, J. P., 1999. "Strength Requirements for Internal and External Prostheses," *J.Biomech.,* Elsevier Science Ltd, **32**(4) pp. 381-393. DOI: 10.1016/S0021-9290(98)00190-0.

[78] Mudali, U. K., Sridhar, T. M., and Baldev, R. A. J., 2003. "Corrosion of Bio Implants," *Sadhana - Academy Proceedings in Engineering Sciences,* **28**(3-4) pp. 601-637.

[79] Fregly, B. J., Sawyer, W. G., Harman, M. K., and Banks, S. A., 2005. "Computational Wear Prediction of a Total Knee Replacement from in Vivo Kinematics," *Journal of Biomechanics,* **38**(2) pp. 305-314. DOI: 10.1016/j.jbiomech.2004.02.013.

[80] Alhassan, S., and Goswami, T., 2008. "Wear Rate Model for UHMWPE in Total Joint Applications," *Wear,* **265**(1-2) pp. 8-13. DOI: 10.1016/j.wear.2007.08.017.

[81] Goswami, T., and Alhassan, S., 2008. "Wear Rate Model for UHMWPE in Total Hip and Knee Arthroplasty," *Materials & Design,* **29**(2) pp. 289-296. DOI: 10.1016/j.matdes.2007.02.015.

[82] Skripitz, R., and Aspenberg, P., 1998. "Tensile Bond between Bone and Titanium. A Reappraisal of Osseointegration," *Acta Orthopaedica Scandinavica,* **69**(3) pp. 315-319.

[83] Nielsen, P. T., Hansen, E. B., and Rechnagel, K., 1992. "Cementless Total Knee Arthroplasty in Unselected Cases of Osteoarthritis and Rheumatoid Arthritis: A 3-Year Follow-Up Study of 103 Cases," *The Journal of Arthroplasty,* **7**(2) pp. 137-143. DOI: 10.1016/0883-5403(92)90006-C.

[84] Rakotomanana, R. L., Leyvraz, P. F., Curnier, A., Heegaard, J. H., and Rubin, P. J., 1992. "A Finite Element Model for Evaluation of Tibial Prosthesis-Bone Interface in Total Knee Replacement," *Journal of Biomechanics,* **25**(12) pp. 1413-1424. DOI: 10.1016/0021-9290(92)90055-6.

[85] Van Rietbergen, B., Huiskes, R., Weinans, H., Sumner, D. R., Turner, T. M., and Galante, J. O., 1993. "The Mechanism of Bone Remodeling and Resorption Around Press-Fitted Total Hip Arthroplasty Stems," *Journal of Biomechanics,* **26**(4-5) pp. 369-382.

[86] Van Lenthe, G. H., Willems, M. M. M., Verdonschot, N., De Waal Malefijt, M. C., and Huiskes, R., 2002. "Stemmed Femoral Knee Prostheses: Effects of Prosthetic Design and Fixation on Bone Loss," *Acta Orthopaedica Scandinavica,* **73**(6) pp. 630-637.

[87] Goswami, T., 2003. "Fatigue Crack Growth Behavior of Ti-6Al-4V Alloy Forging," *Materials and Design,* **24**(6) pp. 423-433.

[88] American Association of Hip and Knee Surgeons, 2007. "Knee Implants," *www.aaos.org.* American Academy of Orthopaedic Surgeons, Accessed June 1, 2010, <http://orthoinfo.aaos.org/topic.cfm?topic=A00389>.

[89] Lombardi, A. V., Mallory, T. H., Staab, M., and Herrington, S. M., 1998. "Particulate Debris Presenting as Radiographic Dense Masses Following Total Knee Arthroplasty." *The Journal of Arthroplasty,* **13**(3) pp. 351-351-5.

[90] Adam, F., Hammer, D. S., Pfautsch, S., and Westermann, K., 2002. "Early Failure of a Press-Fit Carbon Fiber Hip Prosthesis with a Smooth Surface," *The Journal of Arthroplasty,* **17**(2) pp. 217-223.

[91] Pilliar, R. M., Lee, J. M., and Maniatopoulos, C., 1986. "Observations on the Effect of Movement on Bone Ingrowth into Porous-Surfaced Implants," *Clinical Orthopaedics and Related Research,* **208** pp. 108-113.

[92] Hamlin, F. D., Buechel, F. F., and Pappas, M. J., 1993. "Stress Shielding as it Relates to Proximally Porous Coated Femoral Stems of Varying Configurations: A 10-Year Cementless Total Hip Replacement Study," *Journal of Orthopaedic Rheumatology,* **6**(2-3) pp. 57-70.

[93 Kienapfel, H., Sprey, C., Wilke, A., and Griss, P., 1999. "Implant Fixation by Bone Ingrowth," *The Journal of Arthroplasty,* **14**(3) pp. 355-368.

[94] Schrøder, H. M., Berthelsen, A., Hassani, G., Hansen, E. B., and Solgaard, S., 2001. "Cementless Porous-Coated Total Knee Arthroplasty: 10-Year Results in a Consecutive Series," *The Journal of Arthroplasty,* **16**(5) pp. 559-567. DOI: 10.1054/arth.2001.23565.

[95] Cameron, H. U., and Cameron, G., 1987. "Stress-Relief Osteoporosis of the Anterior Femoral Condyles in Total Knee Replacement. A Study of 185 Patients." *Orthopaedic Review,* **16**(7) pp. 449-456.

[96] Ebert, F. R., Krackow, K. A., Lennox, D. W., Hungerford, D. S., 1992. "Minimum 4-year follow-up of the PCA total knee arthroplasty in rheumatoid patients," *Journal of Arthroplasty,* **7**(1) pp. 101-108.

[97] Au, A. G., James Raso, V., Liggins, A. B., and Amirfazli, A., 2007. "Contribution of Loading Conditions and Material Properties to Stress Shielding Near the Tibial Component of Total Knee Replacements," *Journal of Biomechanics,* **40**(6) pp. 1410-1416. DOI: 10.1016/j.jbiomech.2006.05.020.

[98] Frost, H. M., 1990. "Skeletal structural adaptations to mechanical usage (SATMU): 1. Redefining Wolff's law: The bone modeling problem," *Anatomical Record,* **226**(4) pp.:403-413.

[99] Fischer, K. J., 1994. "Correspondence between Bone Density Distributions and Mechanical Loading," *Mechanical Engineering,* Stanford, CA, Stanford University.

[100] Marcus, R., 1987. "Normal and abnormal bone remodeling in man," *Annual Review of Medicine,* **38** pp. 129-141.

[101] Humphrey, G. M., 1858. "*A treatise of the human skeleton*," 1st Edition, Macmillan and Co., London.

[102] Awode, M. R., 2005. "*Nonequilibrium thermodynamics: irreversible thermodynamics of physico-chemical and biological processes*," 1st edition, Nagpur: Dattsons, 141 p. ISBN: 9788171920631

[103] Treharne, R. W., 1981. "Review of Wolff's Law and its Proposed Means of Operation," *Orthopaedic Review,* **10**(1) pp. 35-47.

[104] Cowin, S. C., 1986. "Wolff's Law of Trabecular Architecture at Remodeling Equilibrium," *Journal of Biomechanical Engineering,* **108**(1) pp. 83-88.

[105] Lanyon, L. E., 1974. "Experimental support for the trajectorial theory of bone structure," *Journal of Bone and Joint Surgery - Series B* **56**(1) pp. 160-166.

[106] Frost, H., 1986. "*Intermediary organization of the skeleton,*" Boca Raton, FL: CRC press

[107] Cowin, S. C., Hegedus, D. H., 1976. "Bone remodeling I: theory of adaptive elasticity," *Journal of Elasticity,* **6**(3) pp. 313-326.

[108] Cowin, S. C., Nachlinger, R. R., 1978. "Bone remodeling III: uniqueness and stability in adaptive elasticity theory," *Journal of Elasticity,* **8** (3) pp. 285-295.

[109] Hart, R. T., Davy, D. T., Heiple, K. G., 1984. "A computational method for stress analysis of adaptive elastic materials with a view toward applications in strain-induced bone remodeling," *Journal of Biomechanical Engineering,* **106** (4) pp. 342-350.

[110] Fyhrie, D. P., Carter, D. R., 1986. "A unifying principle relating stress to trabecular bone morphology," *Journal of Orthopaedic Research,* **4**(3) pp. 304-317.

[111] Cowin, S. C., 1981. "Continuum models of the adaptation of bone to stress," *American Society of Mechanical Engineers, Applied Mechanics Division, AMD* **45** pp. 193-210.

[112] Hart, R. T., 1983. "Quantitative response of bone to mechanical stress," P.h.D thesis, Department of Mechanical and Aerospace Engineering, Case Western Reserve University, Cleveland, Ohio.

[113] Huiskes, R., Dalstra, M., Vondervenne, R., Grootenboer, H., Slooff, T. J., 1987. "A hypothesis concerning the effect of implant rigidity on adaptive cortical bone remodeling in the femur," *Journal of Biomechanics,* **20** (8) pp. 808-809.

[114] Hart, R. T., Davy, D. T., 1989. "Theories of bone modeling and remodeling" *Bone Mechanics*, pp. 253-77.

[115] Frost, H. M., 1987. "Bone 'mass' and the 'mechanostat': A proposal," *Anatomical Record,* **219** (1) pp. 1-9.

[116] Hernandez, C. J., Beaupré, G. S., Carter, D. R., 2000. "A model of mechanobiologic and metabolic influences on bone adaptation," *Journal of Rehabilitation Research and Development,* **37** (2) pp. 235-244.

[117] Kroll, M. H., 2000. "Parathyroid hormone temporal effects on bone formation and resorption," *Bulletin of Mathematical Biology,* **62**(1) pp. 163-188.

[118] Rattanakul, C., Lenbury, Y., Krishnamara, N., Wollkind, D. J., 2003. "Modeling of bone formation and resorption mediated by parathyroid hormone: Response to estrogen/PTH therapy," *BioSystems,* **70**(1) pp. 55-72.

[119] Mundy, G. R., 1995. "*Bone Remodeling and Its Disorders*" 2nd edition, Martin Dunitz, London, 216 p. ISBN: 185317257X

[120] Hofbauer, L. C., Heufelder, A. E., 2001. "Role of receptor activator of nuclear factor-κB ligand and osteoprotegerin in bone cell biology," *Journal of Molecular Medicine*, **79**(5-6) pp. 243-253.

[121] Raisz, L. G., 1999. "Physiology and pathophysiology of bone remodeling," *Clinical Chemistry*, **45**(8 II) pp. 1353-1358.

[122] Mundy, G. R., Roodman, G. D., 1987. "Osteoclast ontogeny and function," *Bone and Mineral Research*, **5** pp. 209-279.

[123] Bougherara, H., Bureau, M. N., Yahia, L., 2010. "Bone remodeling in a new biomimetic polymer-composite hip stem," *Journal of Biomedical Materials Research - Part A*, **92**(1) pp. 164-174.

[124] Carter, D. R., Orr, T. E., Fyhrie, D. P., 1989. "Relationships between loading history and femoral cancellous bone architecture," *Journal of Biomechanics* **22**(3) pp. 231-244.

[125] Weinans, H., R. Sumner, D., Igloria, R., Natarajan, R. N., 2000. "Sensitivity of periprosthetic stress-shielding to load and the bone density-modulus relationship in subject-specific finite element models," *Journal of Biomechanics*, **33**(7) pp. 809-817.

[126] Fung, Y. C., 1990. "*Biomechanics: motion, flow, stress, and growth*," New York: Springer-Verlag, 569 p., ISBN: 0387971246.

[127] Yourgrau, W., 1982. "*Treatise on irreversible and statistical thermophysics: an introduction to nonclassical thermodynamics*," New York: Dover, 268 p., ISBN: 0486495191

[128] Ignetik, R., Deakin, M. A. B., 1981. "Asymptotic analysis of the Michaelis-Menten reaction equations," *Bulletin of Mathematical Biology*, **43**(4) pp. 375-388.

[129] Nicolis, G., 1979. "Irreversible thermodynamics," *Reports on Progress in Physics*, **42**(2), art. no. 001, pp. 225-268.

[130] Mohammed, R. H. F., 2008. "Orders of Reaction:Orders of Reaction and Rate Equations & Mechanisms," Version 2. Knol. 2008 Nov 18. Accessed July 5, 2010, http://knol.google.com/k/prof-dr-amgad-mohammed-rabie-hamed/orders-of-reaction/yjz2w4zqxavw/8.

[131] Kuhl, E., Balle., F., 2005. "Computational modeling of hip replacement surgery: Total hip replacement vs. hip resurfacing," *Technische Mechanik*, **25**(2) pp. 107-114.

[132] Reilly, D. T., and Burstein, A. H., 1975. "The Elastic and Ultimate Properties of Compact Bone Tissue," *Journal of Biomechanics,* **8**(6) pp. 393-396. DOI: 10.1016/0021-9290(75)90075-5.

[133] Williams, J. L., and Lewis, J. L., 1982. "Properties and an Anisotropic Model of Cancellous Bone from the Proximal Tibial Epiphysis," *Journal of Biomedical Engineering*, **104**(1) pp. 50-56.

[134] Zdero, R., Olsen, M., Bougherara, H., and Schemitsch, E. H., 2008. "Cancellous Bone Screw Purchase: A Comparison of Synthetic Femurs, Human Femurs, and Finite Element Analysis," *Proceedings of the Institution of Mechanical Engineers - Part H: Journal of Engineering in Medicine,* **222** pp. 1175-1183(9).

[135] Papini, M., Zdero, R., Schemitsch, E. H., and Zalzal, P., 2007. "The Biomechanics of Human Femurs in Axial and Torsional Loading: Comparison of Finite Element Analysis, Human Cadaveric Femurs, and Synthetic Femurs," *Journal of Biomechanical Engineering,* **129**(1) pp. 12-19.

[136] Stryker Corporation, 2010. "Duracon Total Stabilizer Knee System," *Stryker.com (Stryker Orthopaedics: Knee Replacement System).* Stryker Corporation, Kalamazoo, MI. Accessed July, 6,2010,http://www.stryker.com/en-us/products/Orthopaedics/KneeReplacement/Revision/DuraconTS/index.htm#

[137] eFunda, I., "Pure Elements: Element Listing (Cobalt, Chromium, Molybdenum)," *Engineering Fundamentals (efunda.com): Materials Home.* eFunda, Inc, Sunnyvale, CA. Accessed May 15, 2010, http://www.efunda.com/materials/elements/element_list.cfm.

[138] Suedam, V., Souza, E. A. C., Moura, M. S., Jacques, L. B., and Rubo, J. H., 2009. "Effect of Abutment's Height and Framework Alloy on the Load Distribution of Mandibular Cantilevered Implant-Supported Prosthesis," *Clinical Oral Implants Research,* **20**(2) pp. 196-200. DOI: 10.1111/j.1600-0501.2008.01609.x.

[139] Rubin, C. T., Lanyon, L. E., 1985. "Regulation of bone mass by mechanical strain magnitude," *Calcified Tissue International*, **37**(4) pp. 411-417.

[140] ANSYS Inc, 2009. "SOLID187 3-D 10-Node Tetrahedral Structural Solid," *kxcad.net; Release 11.0 Documentation for ANSYS.* Accessed May 11, 2010, http://www.kxcad.net/ansys/ANSYS/ansyshelp/Hlp_E_SOLID187.html#solid187.tab.2.ft.6.

[141] ANSYS Inc, 2005. "CONTA174 3-D 8-Node Surface-to-Surface Contact," *University of Illinois at Chicago Academic Computing and Communications Centre.* Accessed May 11, 2010, http://uic.edu/depts/accc/software/ansys/html/elem_55/chapter4/ES4-174.htm.

[142] ANSYS Inc, 2009. "TARGE170 3-D Target Segment," *kxcad.net; Release 11.0 Documentation for ANSY.* Accessed May 11, 2010, http://www.kxcad.net/ansys/ANSYS/ansyshelp/Hlp_E_TARGE170.html

[143] ANSYS Inc, 2005. "TARGE170 3-D Target Segment," *University of Illinois at Chicago Academic Computing and Communications Centre.* Accessed May 11, 2010, http://uic.edu/depts/accc/software/ansys/html/elem_55/chapter4/ES4-170.htm

[144] SciELO, 2010. "Scientific Electronic Library," Accessed July 15, 2010, http://www.scielo.br/img/revistas/mioc/v101s2/v101s2a15f24.gif

[145] Sanchis-Alfonso V., 2006. "*Anterior knee pain and patellar instability*," electronic resource, London: Springer Verlog.

[146] Van Loon, C. J. M., Oyen, W. J. G., deWaal Malefijt, M. C., and Verdonschot, N., 2001. "Distal Femoral Bone Mineral Density After Total Knee Arthroplasty: A Comparison with General Bone Mineral Density," *Archives of Orthopaedic and Trauma Surgery*, Springer-Verlag, **121**(5) pp. 282-285.